several decades to evolve (El-Serag, 2011). Currently, HCC is the third most deadly and fifth most common cancer worldwide, and in the United States its incidence has doubled in the past two decades. Furthermore, 8% of the world's population are chronically infected with hepatitis B or C viruses (HBV and HCV) and are at a high risk of new HCC development (El-Serag, 2011). Up to 5% of HCV patients will develop HCC in their lifetime, and the yearly HCC incidence in patients with cirrhosis is 3%–5%. These tumors may arise from premalignant lesions, ranging from dysplastic foci to dysplastic hepatocyte nodules that are often seen in damaged and cirrhotic livers and are more proliferative than the surrounding parenchyma (Hytiroglou et al., 2007). However, the tumorigenic potential of these lesions was never examined, and it is unknown whether they contain any genetic alterations. Given that there is no effective treatment for HCC and, upon diagnosis, most patients with advanced disease have a remaining lifespan of 4–6 months, it is important to detect HCC early, while it is still amenable to surgical resection or chemotherapy. Premalignant lesions, called foci of altered hepatocytes (FAH), were also described in chemically induced HCC models (Pitot, 1990), but it was questioned whether these lesions harbor tumor progenitors or result from compensatory proliferation (Sell and Leffert, 2008). The aim of this study was to determine whether HCC progenitor cells (HcPCs) exist and if so, to isolate these cells and identify some of the signaling networks that are involved in their maintenance and progression.

We now describe HcPC isolation from mice treated with the procarcinogen diethyl nitrosamine (DEN), which induces poorly differentiated HCC nodules within 8 to 9 months (Verna et al., 1996). Although these tumors do not evolve in the context of cirrhosis, the use of a chemical carcinogen is justified because the finding of up to 121 mutations per HCC genome suggests that carcinogens may be responsible for human HCC induction (Guichard et al., 2012). Furthermore, 20%–30% of HCC, especially in HBV-infected individuals, evolve in noncirrhotic livers (El-Serag, 2011). Nonetheless, we also isolated HcPCs from *Tak1*$^{\Delta hep}$ mice, which develop spontaneous HCC as a result of progressive liver damage, inflammation, and fibrosis caused by ablation of TAK1 (Inokuchi et al., 2010). Although the etiology of each model is distinct, both contain HcPCs that express marker genes and signaling pathways previously identified in human HCC stem cells (Marquardt and Thorgeirsson, 2010) long before visible tumors are detected. Furthermore, DEN-induced premalignant lesions and HcPCs exhibit autocrine IL-6 production that is critical for tumorigenic progression. Circulating IL-6 is a risk indicator in several human pathologies and is strongly correlated with adverse prognosis in HCC and cholangiocarcinoma (Porta et al., 2008; Soresi et al., 2006). IL-6 produced by in-vitro-induced CSCs was suggested to be important for their maintenance (Iliopoulos et al., 2009). Furthermore, autocrine IL-6 was detected in several cancers, but its origin is poorly understood (Grivennikov and Karin, 2008). In particular, little is known about the source of IL-6 in HCC. In early stages of hepatocarcinogenesis, IL-6 is produced by Kupffer cells or macrophages (Maeda et al., 2005; Naugler et al., 2007). However, paracrine IL-6 production is transient and does not explain its expression by HCC cells.

RESULTS

DEN-Induced Collagenase-Resistant Aggregates of HCC Progenitors

A single intraperitoneal (i.p.) injection of DEN into 15-day-old BL/6 mice induces HCC nodules first detected 8 to 9 months later. However, hepatocytes prepared from macroscopically normal livers 3 months after DEN administration already contain cells that progress to HCC when transplanted into the permissive liver environment of MUP-uPA mice (He et al., 2010), which express urokinase plasminogen activator (uPA) from a mouse liver-specific major urinary protein (MUP) promoter and undergo chronic liver damage and compensatory proliferation (Rhim et al., 1994). Collagenase digestion of DEN-treated livers generated a mixture of monodisperse hepatocytes and aggregates of tightly packed small hepatocytic cells (Figure 1A). Aggregated cells were also present—but in lower abundance—in digests of control livers (Figure S1A available online). HCC markers such as α fetoprotein (AFP), glypican 3 (Gpc3), and Ly6D, whose expression in mouse liver cancer was reported (Meyer et al., 2003), were upregulated in aggregates from DEN-treated livers, but not in nonaggregated hepatocytes or aggregates from control livers (Figure S1A). Thus, control liver aggregates may result from incomplete collagenase digestion, whereas aggregates from DEN-treated livers may contain HcPC. DEN-induced aggregates became larger and more abundant 5 months after carcinogen exposure, when they consisted of 10–50 cells that were smaller than nonaggregated hepatocytes. Using 70 μm and 40 μm sieves, we separated aggregated from nonaggregated hepatocytes (Figure 1A) and tested their tumorigenic potential by transplantation into MUP-uPA mice (Figure 1B). To facilitate transplantation, the aggregates were mechanically dispersed and suspended in Dulbecco's modified Eagle's medium (DMEM). Five months after intrasplenic (i.s.) injection of 10^4 viable cells, mice receiving cells from aggregates developed about 18 liver tumors per mouse, whereas mice receiving nonaggregated hepatocytes developed less than 1 tumor each (Figure 1B). The tumors exhibited typical trabecular HCC morphology and contained cells that abundantly express AFP (Figure S1B). To confirm that the HCCs were derived from transplanted cells, we measured their relative MUP-uPA DNA copy number and found that they contained much less MUP-uPA transgene DNA than the surrounding parenchyma (Figure S1C). Transplantation of aggregated cells from livers of DEN-treated actin-GFP transgenic mice resulted in GFP-positive HCCs (Figure S1D). Both experiments strongly suggest that the HCCs were derived from the transplanted cells. No tumors were ever observed after transplantation of control hepatocytes (nonaggregated or aggregated).

Only liver tumors were formed by the transplanted cells. Other organs, including the spleen into which the cells were injected, remained tumor free (Figure 1B), suggesting that HcPCs progress to cancer only in the proper microenvironment. Indeed, no tumors appeared after HcPC transplantation into normal BL/6 mice. But, if BL/6 mice were first treated with retrorsine (a chemical that permanently inhibits hepatocyte proliferation [Laconi et al., 1998]), intrasplenically transplanted with HcPC-containing aggregates, and challenged with CCl_4 to induce liver injury and compensatory proliferation (Guo et al., 2002), HCCs readily

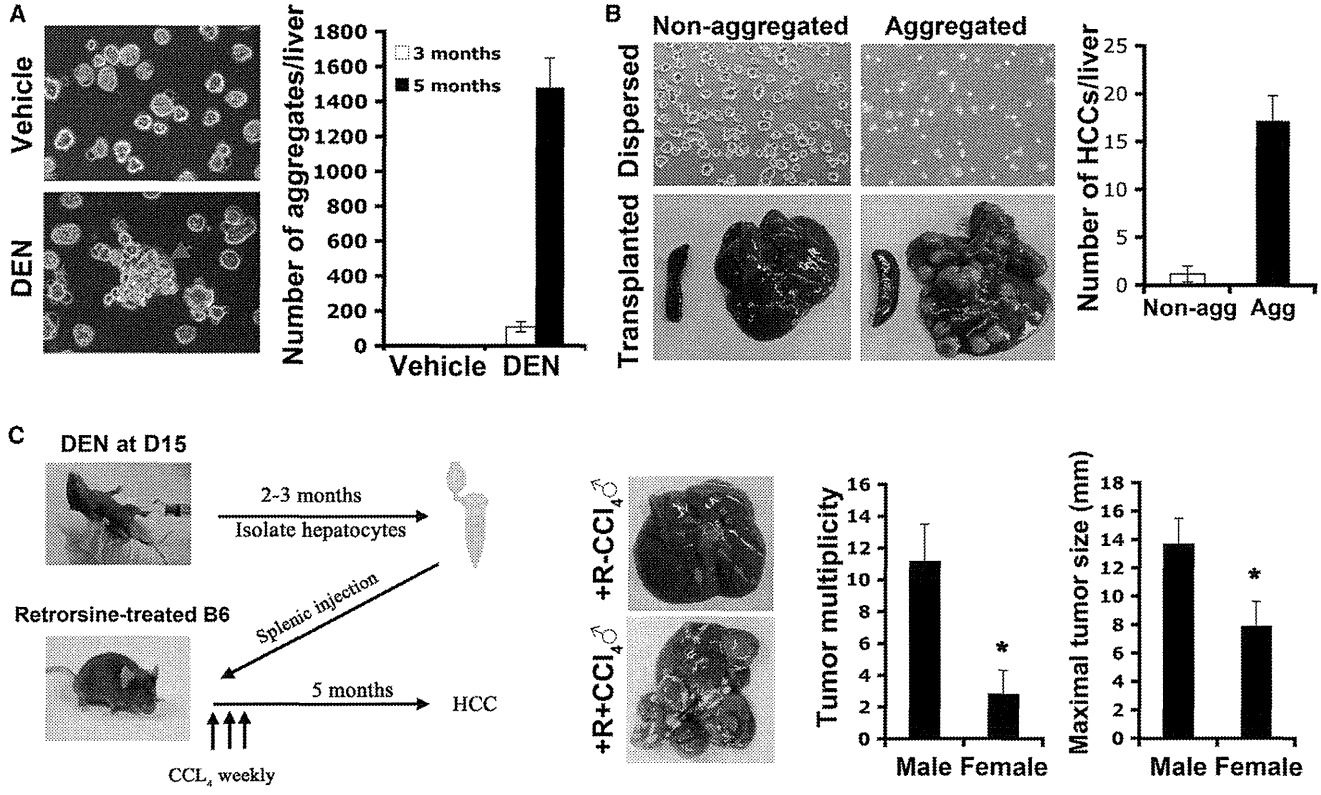

E

Type of cells	Number of cells transplanted			
	$4x10^4$	$1X10^4$	1000	100
Unsorted	2(2)	9(9)	2(5)	0(3)
$CD44^+$	nd	nd	4(4)	2(4)
$CD44^-$	nd	nd	0(4)	0(5)

Figure 1. DEN-Induced Hepatocytic Aggregates Contain $CD44^+$ HCC Progenitors

(A) Fifteen-day-old BL/6 males were given DEN or vehicle. After 3 or 5 months, their livers were removed and collagenase digested. Left: typical digest appearance (magnification: 400×; 3 months after DEN). Red arrow indicates a collagenase-resistant aggregate. Right: aggregates per liver (n = 5; ± SD for each point).

(B) Livers were collagenase digested 5 months after DEN administration. Aggregates were separated from nonaggregated cells and mechanically dispersed into a single-cell suspension (left upper panels; 200×). 10^4 viable aggregated or nonaggregated cells were i.s. injected into MUP-uPA mice whose livers and spleens were analyzed for tumors 5 months later (left lower panels). The number of HCC nodules per liver was determined (n = 5; ± SD).

(C) Adult BL/6 mice were given retrorsine twice with a 2 week interval to inhibit hepatocyte proliferation. After 1 month, mice were i.s. transplanted with dispersed hepatocyte aggregates (10^4 cells) from DEN-treated mice and, 2 weeks later, were given three weekly i.p. injections of CCl_4 or vehicle. Tumor multiplicity and size were evaluated 5 months later (n = 5; ± SD).

(D) Hepatocyte aggregates were prepared as in (A), stained with CD44 antibody and DAPI, and examined by fluorescent microscopy (400×).

(E) Hepatocyte aggregates were dispersed as above, and $CD44^+$ cells were separated from $CD44^-$ cells. The indicated cell numbers were injected into MUP-uPA mice, and HCC development was evaluated 5 months later. n values are in parentheses (n.d., not done).

See also Figure S1.

appeared (Figure 1C). CCl_4 omission prevented tumor development. Notably, MUP-uPA or CCl_4-treated livers are fragile, rendering direct intrahepatic transplantation difficult. The transplanted HcPC-containing aggregates formed more numerous and larger HCC nodules in male recipients than in females (Figure 1C), as observed in MUP-uPA mice transplanted with unfractionated DEN-exposed hepatocytes (He et al., 2010). Thus, CCl_4-induced liver damage, especially within a male liver, generates a microenvironment that drives HcPC proliferation and malignant progression. To examine this point, we transplanted GFP-labeled HcPC-containing aggregates into retrorsine-treated BL/6 mice and examined their ability to proliferate with or without subsequent CCl_4 treatment. Indeed, the GFP^+ cells formed clusters that grew in size only in CCl_4-treated host livers

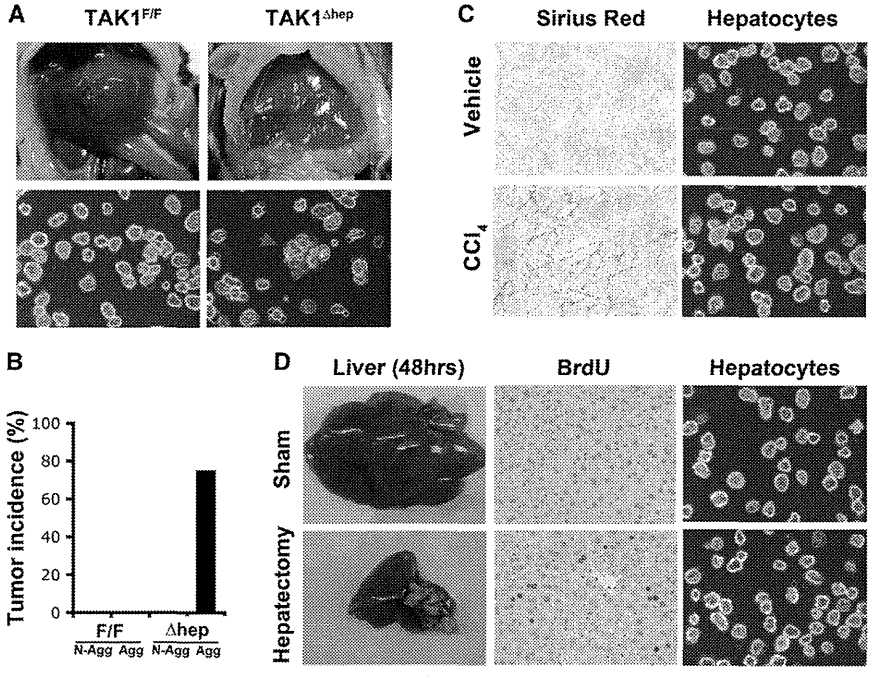

Figure 2. *Tak1*$^{\Delta hep}$ Livers Contain Collagenase-Resistant HcPC Aggregates

(A) Livers, free of tumors (upper panels), were removed from 1-month-old *Tak1*$^{F/F}$ and *Tak1*$^{\Delta hep}$ males and collagenase digested (lower panels; red arrow indicates collagenase-resistant aggregate).

(B) 10^4 nonaggregated or dispersed aggregated hepatocytes from (A) were i.s. injected into MUP-uPA mice that were analyzed 6 months later to identify mice with at least one liver tumor (n = 5–8 mice per genotype).

(C) BL/6 males were injected with vehicle or CCl_4 twice weekly for 2 weeks. Hepatocytes were isolated by collagenase digestion and photographed (right panels; 400×). Liver sections were stained with Sirius red to reveal collagen deposits (left panels).

(D) 8-week-old BL/6 males were subjected to 70% partial hepatectomy, pulsed with BrdU at 46 and 70 hr, and sacrificed 2 hr later. Isolated hepatocytes were photographed. Liver sections were analyzed for BrdU incorporation (400×). See also Figure S2 and Table S1.

(Figure S1E). Omission of $CC1_4$ prevented their expansion. Unlike HCC-derived cancer cells (dih10 cells), which form subcutaneous (s.c.) tumors with HCC morphology (He et al., 2010; Park et al., 2010), the HcPC-containing aggregates did not generate s.c. tumors in BL/6 mice (Figure S1F).

Despite their homogeneous appearance, the HcPC-containing aggregates contained both $CD44^+$ and $CD44^-$ cells (Figure 1D). Because CD44 is expressed by HCC stem cells (Yang et al., 2008; Zhu et al., 2010), we dispersed the aggregates and separated $CD44^+$ from $CD44^-$ cells and transplanted both into MUP-uPA mice. Whereas as few as 10^3 $CD44^+$ cells gave rise to HCCs in 100% of recipients, no tumors were detected after transplantation of $CD44^-$ cells (Figure 1E). Remarkably, 50% of recipients developed at least one HCC after receiving as few as 10^2 $CD44^+$ cells. Mature $CD44^-$ hepatocytes were found to engraft as well as or better than $CD44^+$ small hepatocytic cells (Haridass et al., 2009; Ichinohe et al., 2012). Hence, livers of DEN-treated mice contain $CD44^+$ HcPC that can be successfully isolated and purified and give rise to HCCs after transplantation into appropriate hosts. Unlike fully transformed HCC cells, HcPCs only give rise to tumors within the liver.

HcPC-Containing Aggregates in *Tak1*$^{\Delta hep}$ Mice

We applied the same HcPC isolation protocol to *Tak1*$^{\Delta hep}$ mice, which develop HCC of different etiology from DEN-induced HCC. Importantly, *Tak1*$^{\Delta hep}$ mice develop HCC as a consequence of chronic liver injury and fibrosis without carcinogen or toxicant exposure (Inokuchi et al., 2010). Indeed, whole-tumor exome sequencing revealed that DEN-induced HCC contained about 24 mutations per 10^6 bases (Mb) sequenced, with *B-Raf*^{V637E} being the most recurrent, whereas 1.4 mutations per Mb were detected in *Tak1*$^{\Delta hep}$ HCC's exome (Table S1). By contrast, *Tak1*$^{\Delta hep}$ HCC exhibited gene copy number changes. Collagenase digests of 1-month-old *Tak1*$^{\Delta hep}$ livers contained much more hepatocytic aggregates than *Tak1*$^{f/f}$ liver digests (Figure 2A). Notably, HCC developed in 75% of MUP-uPA mice that received dispersed *Tak1*$^{\Delta hep}$ aggregates, but no tumors appeared in mice receiving nonaggregated *Tak1*$^{\Delta hep}$ or total *Tak1*$^{f/f}$ hepatocytes (Figure 2B). Because *Tak1*$^{\Delta hep}$ mice are subject to chronic liver damage and consequent compensatory proliferation, we wanted to ascertain that the HcPCs are not simply proliferating hepatocytes or expanding bipotential hepatobiliary progenitors using CCl_4 to induce liver injury and compensatory proliferation in WT mice. Although this treatment caused acute liver fibrosis, it did not augment formation of collagenase-resistant aggregates (Figure 2C). Similarly, few aggregates were detected in collagenase digests of livers after partial hepatectomy (Figure 2D). However, bile duct ligation (BDL) or feeding with 3,5-dicarbethoxy-1,4-dihydrocollidine (DDC), treatments that cause cholestatic liver injuries and oval cell expansion (Dorrell et al., 2011), did increase the number of small hepatocytic cell aggregates (Figure S2A). Nonetheless, no tumors were observed 5 months after injection of such aggregates into MUP-uPA mice (Figure S2B). Thus, not all hepatocytic aggregates contain HcPCs, and HcPCs only appear under tumorigenic conditions.

The HcPC Transcriptome Is Similar to that of HCC and Oval Cells

To determine the relationship between DEN-induced HcPCs, normal hepatocytes, and fully transformed HCC cells, we analyzed the transcriptomes of aggregated and nonaggregated hepatocytes from male littermates 5 months after DEN administration, HCC epithelial cells from DEN-induced tumors, and normal hepatocytes from age- and gender-matched littermate controls. Clustering analysis distinguished the HCC samples from other samples and revealed that the aggregated

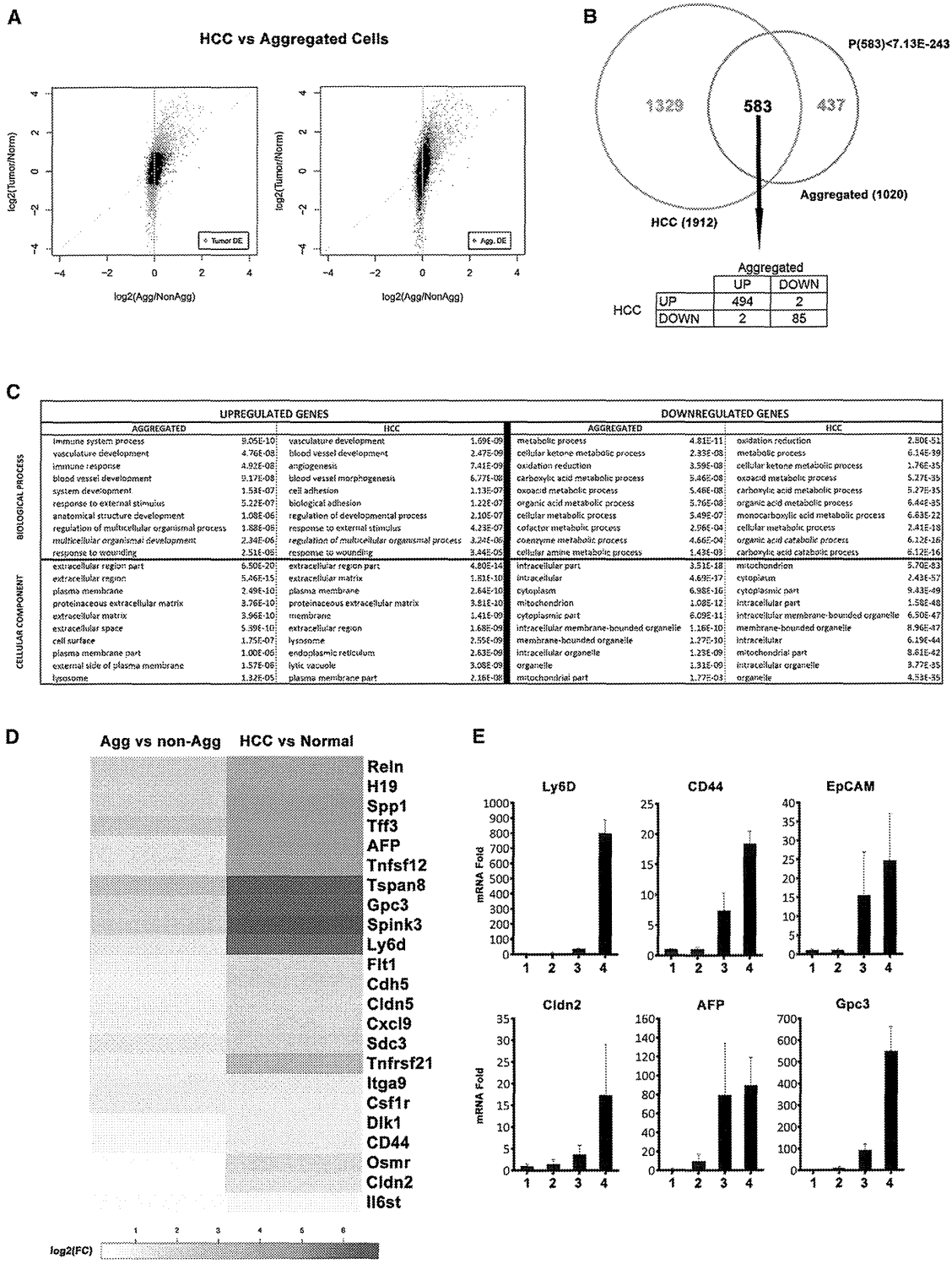

Figure 3. Aggregated Hepatocytes Exhibit an Altered Transcriptome Similar to that of HCC Cells

Aggregated and matched nonaggregated hepatocytes were isolated 5 months after DEN treatment. HCC cells were isolated from DEN-induced tumors, and normal hepatocytes were from age- and gender-matched control mice. RNA was extracted and subjected to microarray analysis (n = 3 for each sample).

(A) Scatterplot representing fold changes (log 2 of expression ratio) in gene expression for HCC versus normal (y axis) and aggregated versus nonaggregated (x axis) pairwise transcriptome comparisons. The plot is displayed twice: in the left panel, genes with an FDR < 0.01 in the aggregated versus nonaggregated

(legend continued on next page)

hepatocyte samples did not cluster with each other but rather with nonaggregated hepatocytes derived from the same mouse (Figure S3A). Interestingly, the aggregated cell transcriptome appeared closer to that of normal hepatocytes than to the HCC profile. This similarity may be due to the presence of ~70% nontumorigenic (or $CD44^-$) hepatocytes within the purified aggregates (Figure 1D). Comparison of the HCC and normal hepatocyte transcriptomes revealed 1,912 differentially expressed genes (false discovery rate [FDR] < 0.01; Figure 3A, left, cyan dots). A similar comparison revealed 1,020 genes that are differentially expressed between aggregated and nonaggregated hepatocytes (FDR < 0.01; Figure 3A, right, red dots). The range of differential expression is wider for the HCC and normal hepatocyte pair than the aggregate versus nonaggregate pair, reflecting presence of normal, nontransformed hepatocytes within the aggregates, resulting in signal dilution. Interestingly, 57% (583/1,020) of genes differentially expressed in aggregated relative to nonaggregated hepatocytes are also differentially expressed in HCC relative to normal hepatocytes (Figure 3B, top), a value that is highly significant ($p < 7.13 \times 10^{-243}$). More specifically, 85% (494/583) of these genes are overexpressed in both HCC and HcPC-containing aggregates (Figure 3B, bottom table). Thus, hepatocyte aggregates isolated 5 months after DEN injection contain cells that are related in their gene expression profile to HCC cells isolated from fully developed tumor nodules.

To gain insight into the functional differences between the transcriptomes of the four populations, we examined which biological processes or cellular compartments were significantly overrepresented in the induced or repressed genes in both pairwise comparisons (Gene Ontology Analysis). As expected, processes and compartments that were enriched in aggregated hepatocytes relative to nonaggregated hepatocytes were almost identical to those that were enriched in HCC relative to normal hepatocytes (Figure 3C). Upregulated genes were related to immune response, angiogenesis, development, and wound healing, and many encoded plasma membrane or secreted proteins. By contrast, downregulated genes were highly enriched for metabolic processes, and many of them encoded mitochondrial proteins or had functions associated with differentiated hepatocytes (Figure 3C). Several human HCC markers, including AFP, Gpc3 and H19, were upregulated in aggregated hepatocytes (Figures 3D and 3E). Aggregated hepatocytes also expressed more Tetraspanin 8 (Tspan8), a cell-surface glycoprotein that complexes with integrins and is overexpressed in human carcinomas (Zöller, 2009). Another cell-surface molecule highly expressed in aggregated cells is Ly6D (Figures 3D and 3E). Immunofluorescence (IF) analysis revealed that Ly6D was undetectable in normal liver but was elevated in FAH and ubiquitously expressed in most HCC cells (Figure S3C). A fluorescent-labeled Ly6D antibody injected into HCC-bearing mice specifically stained tumor nodules (Figure S3D). Other cell-surface molecules that were upregulated in aggregated cells included syndecan 3 (Sdc3), integrin α 9 (Itga9), claudin 5 (Cldn5), and cadherin 5 (Cdh5) (Figure 3D). Aggregated hepatocytes also exhibited elevated expression of extracellular matrix proteins (TIF3 and Reln1) and a serine protease inhibitor (Spink3). Elevated expression of such proteins may explain aggregate formation. Aggregated hepatocytes also expressed progenitor cell markers, including the epithelial cell adhesion molecule (EpCAM) (Figure 3E) and Dlk1 (Figure 3D). Elevated expression of cytokines and cytokine receptors was also detected, including tumor necrosis factor superfamily members 12 and 21, colony-stimulating factor 1 receptor, FMS-like tyrosine kinase 1, chemokine (C-X-C motif) ligand 9, the STAT3-activating cytokine osteopontin, IL-6 receptor (IL-6R) signal transducing subunit (gp130), and oncostatin M (OSM) receptor, which also activates STAT3 (Figure 3D).

Aggregated hepatocytes expressed albumin, albeit less than nonaggregated hepatocytes (Figure 4A). Some aggregated cells were positive for cytokeratin 19 (CK19) and A6, markers for bile duct epithelium and oval cells (Figure 4A). Most cells in the DEN-induced aggregates were AFP positive, and some of them expressed EpCAM (Figure 4A). However, not all markers were expressed by every cell within a given aggregate, suggesting that the aggregates contain liver cells that are related to bipotential hepatobiliary progenitors/oval cells as well as more differentiated progeny and normal hepatocytes. To confirm these observations, we compared the HcPC and HCC (Figure 3A) to the transcriptome of DDC-induced oval cells (Shin et al., 2011). This analysis revealed a striking similarity between the HCC, HcPC, and the oval cell transcriptomes (Figure S3B). Despite these similarities, some genes that were upregulated in HcPC-containing aggregates and HCC were not upregulated in oval cells. Such genes may account for the tumorigenic properties of HcPC and HCC.

We examined the aggregates for signaling pathways and transcription factors involved in hepatocarcinogenesis. Many aggregated cells were positive for phosphorylated c-Jun and STAT3 (Figure 4A), transcription factors involved in DEN-induced

comparison are highlighted in red, and in the right panel, genes with an FDR < 0.01 in the HCC versus normal comparison are highlighted in cyan. DE, differentially expressed.

(B) Venn diagram showing overlap between genes that are differentially expressed between aggregated and nonaggregated hepatocytes and between HCC cells and normal hepatocytes with an FDR < 0.01 (cyan and red dots from A). The probability to find 583 overlapping genes is $<7.13 \times 10^{-243}$. From these 583 common genes, only 4 behaved differently.

(C) The ten most enriched biological processes (upper table) and cellular compartments (lower panel) represented by genes that are significantly upregulated (left panel) or downregulated (right panel) in HCC relative to normal hepatocytes (HCC) or in aggregated relative to nonaggregated hepatocytes (aggregated).

(D) Heatmap displaying positive fold changes (FC) in expression of genes of interest in aggregated versus nonaggregated HcPCs (left) and in HCC versus normal hepatocytes (right).

(E) Expression of selected genes was examined by real-time PCR and is depicted as fold change relative to normal hepatocytes given an arbitrary value of 1.0 (n = 3; ± SD). (1) Normal hepatocytes; (2) nonaggregated hepatocytes from DEN-treated liver; (3) HcPC aggregates from DEN-treated liver; and (4) DEN-induced HCCs.

See also Figure S3.

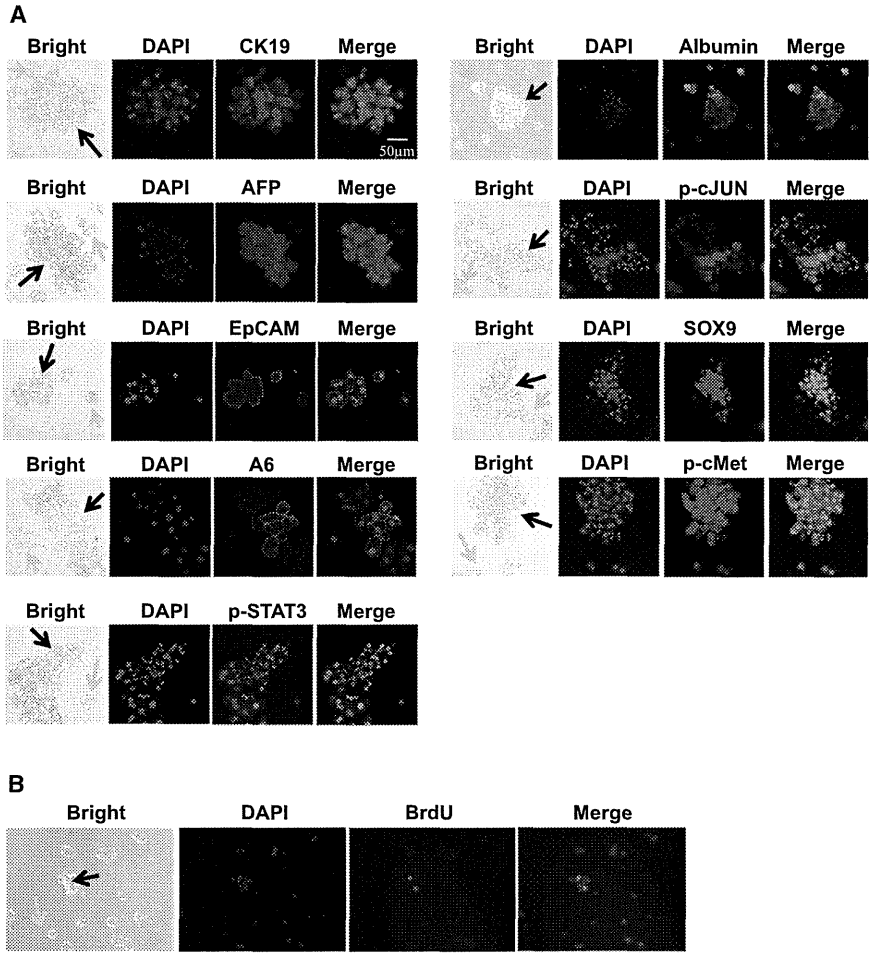

Figure 4. DEN-Induced HcPC Aggregates Express Pathways and Markers Characteristic of HCC and Hepatobiliary Stem Cells

(A) Cytospin preps of collagenase-resistant aggregates from 5-month-old DEN-injected mice were stained with antibodies to CK19, AFP, EpCAM, A6, phospho-Y-STAT3 (Tyr705), albumin, phospho-c-Jun, Sox9, and phospho-c-Met. Black arrows indicate aggregates, and yellow arrows indicate nonaggregated cells (magnification: 400×). (B) 5-month-old DEN-treated mice were injected with BrdU, and 2 hr later, collagenase-resistant aggregates were isolated and analyzed for BrdU incorporation (400×).

See also Figure S4.

hepatocarcinogenesis (Eferl et al., 2003; He et al., 2010). Sox9, a transcription factor that marks hepatobiliary progenitors (Dorrell et al., 2011), was also expressed by many of the aggregated cells, which were also positive for phosphorylated c-Met (Figure 4A), a receptor tyrosine kinase that is activated by hepatocyte growth factor (HGF) and is essential for liver development (Bladt et al., 1995) and hepatocarcinogenesis (Wang et al., 2001). Few of the nonaggregated hepatocytes exhibited activation of these signaling pathways. Aggregates from bromodeoxyuridine (BrdU)-pulsed DEN-treated mice contained BrdU-positive cells (Figure 4B), indicating that they were actively proliferating prior to isolation. Hepatocyte aggregates from 1-month-old *Tak1*$^{\Delta hep}$ mice also contained cells positive for AFP, Sox9, phosphorylated c-Met, and EpCAM, but not A6-positive cells (Figure S4A). Many of the cells also exhibited partially activated β-catenin, phosphorylated STAT3, and phosphorylated c-Jun. Thus, despite different etiology, HcPC-containing aggregates from *Tak1*$^{\Delta hep}$ mice exhibit upregulation of many of the same markers and pathways that are upregulated in DEN-induced HcPC-containing aggregates. Flow cytometry confirmed enrichment of CD44$^+$ cells as well as CD44$^+$/CD90$^+$ and CD44$^+$/EpCAM$^+$ double-positive cells in the HcPC-containing aggregates from either DEN-treated or *Tak1*$^{\Delta hep}$ livers (Figure S4B).

HcPC-Containing Aggregates Originate from Premalignant Dysplastic Lesions

FAH are dysplastic lesions occurring in rodent livers exposed to hepatic carcinogens (Su et al., 1990). Similar lesions are present in premalignant human livers (Su et al., 1997). Yet, it is still debated whether FAH correspond to premalignant lesions or are a reaction to liver injury that does not lead to cancer (Sell and Leffert, 2008). In DEN-treated males, FAH were detected as early as 3 months after DEN administration (Figure 5A), concomitant with the time at which HcPC-containing aggregates were detected. In females, FAH development was delayed. In both genders, FAH were confined to zone 3 and consisted of tightly packed small hepatocytic cells, some of which were proliferative based on BrdU incorporation (Figure 5B). BrdU$^+$ cells were first detected in DEN-treated males and were confined to FAH and rarely detected in age-matched control mice. FAH contained cells positive for the same progenitor cell markers and activated signaling pathways present in HcPC-containing aggregates, including AFP, CD44, and EpCAM (Figure 5C). FAH also contained cells positive for activated STAT3, c-Jun, and PCNA (Figure 5C). Many cells within FAH exhibited strong upregulation of YAP (Figure 5C), a transcriptional coactivator that is negatively regulated by the Hippo pathway and a liver cancer oncoprotein (Zheng et al., 2011). FAH were also enriched in F4/80$^+$ macrophages (Figure 5C). These results suggest that the HcPC-containing aggregates may be derived from FAH.

HcPCs Exhibit Autocrine IL-6 Expression Necessary for HCC Progression

In situ hybridization (ISH) and immunohistochemistry (IHC) revealed that DEN-induced FAH contained IL-6-expressing cells (Figures 6A, 6B, and S5), and freshly isolated DEN-induced aggregates contained more IL-6 messenger RNA (mRNA) than nonaggregated hepatocytes (Figure 6C). We examined several

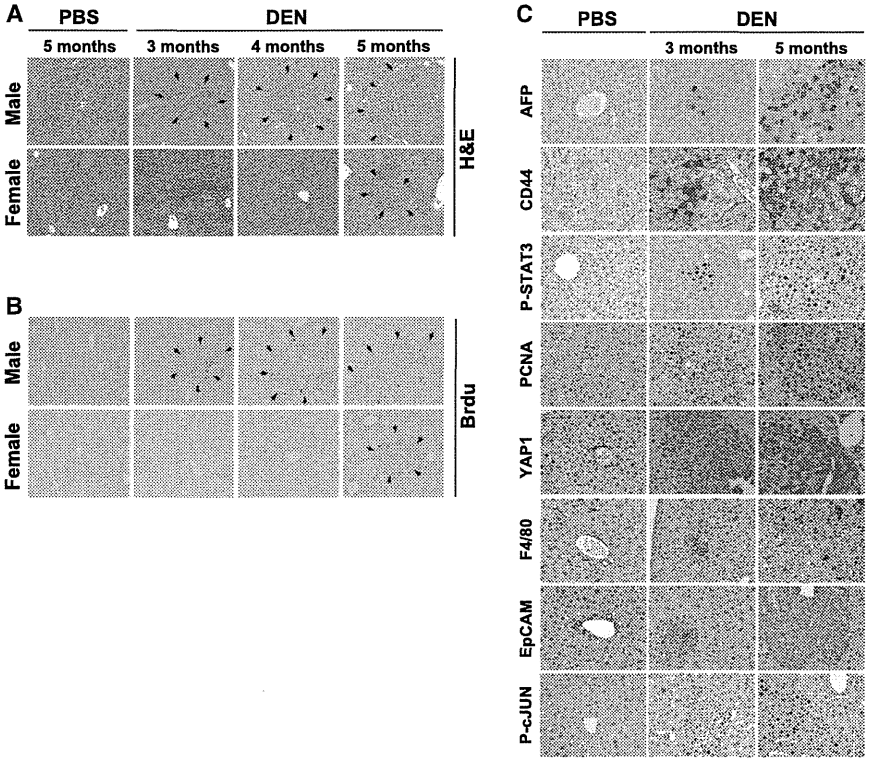

Figure 5. HcPC-Containing Aggregates May Originate from Liver Premalignant Lesions

(A and B) Male and female mice were injected with PBS or DEN at 15 days. At the indicated time points, BrdU was administrated, and livers were collected 2 hr later and stained with H&E (A) or a BrdU-specific antibody (B). Arrows indicate borders of FAH (magnification: 200×).

(C) Sections of male livers treated as above were subjected to IHC with the indicated antibodies (400×).

factors that control IL-6 expression and found that LIN28A and B were significantly upregulated in HcPCs and HCC (Figures 6D and 6E). LIN28-expressing cells were also detected within FAH (Figure 6F). As reported (Iliopoulos et al., 2009), knockdown of LIN28B in cultured HcPC or HCC cell lines decreased IL-6 expression (Figure 6G). LIN28 exerts its effects through downregulation of the microRNA (miRNA) Let-7 (Iliopoulos et al., 2009). Accordingly, miRNA array analysis of aggregated and nonaggregated hepatocytes from DEN-treated mice indicated that the amount of Let-7, along with other miRNAs that also inhibit IL-6 expression (miR194 and miR872), was lower in aggregated cells than in nonaggregated cells (Table S2).

To determine whether autocrine IL-6 production is needed for HCC growth, we silenced IL-6 expression with small hairpin RNA (shRNA) in dih10 HCC cells (He et al., 2010). This resulted in nearly a 75% decrease in IL-6 mRNA (Figure 7A) but had little effect on cell growth in the presence of growth factors, including EGF and insulin (Figure S6A). IL-6 mRNA silencing, however, diminished the ability of dih10 cells to form s.c. tumors (Figures S6B and S6C) and inhibited their ability to form HCCs and proliferate after transplantation into MUP-uPA mice (Figures 7B and S6D). To investigate the importance of autocrine IL-6 production at an earlier step, we isolated HcPC from DEN-treated WT and *Il6*$^{-/-}$ mice. Although IL-6 ablation attenuates HCC induction (Naugler et al., 2007), we still could isolate collagenase-resistant aggregates from livers of DEN-injected *Il6*$^{-/-}$ mice. Notably, IL-6 ablation did not reduce the proportion of CD44^{+} cells in the aggregates (Figures S7A and S7B). We introduced an identical number of WT and *Il6*$^{-/-}$ aggregated hepatocytes into MUP-uPA mice and scored HCC development 5 months later. The IL-6 deficiency resulted in a 2.5-fold decrease in tumorigenic potential (Figure 7C), suggesting that autocrine IL-6 contributes to HcPC to HCC progression. To confirm this point, we dispersed freshly isolated DEN-induced aggregates and transduced them with bicistronic lentiviruses encoding either scrambled or IL-6-specific shRNAs and a GFP marker. After a few days in culture, the transduced cells were introduced into MUP-uPA mice that were examined for HCC development 6 months later. Silencing of IL-6 reduced HCC generation (Figure 7D) and inhibited formation of GFP^{+} colonies within the MUP-uPA liver (Figure 7E). We also ablated IL-6 expression in mouse hepatocytes and found that this led to a marked reduction in DEN-induced tumorigenesis (Figure 7F). Thus, autocrine IL-6 production by DEN-initiated HcPC is important for HCC development. To investigate whether autocrine IL-6 signaling also occurs in human premalignant lesions, we examined needle biopsies of normal liver tissue and HCV-infected livers with dysplastic lesions. We found that 16% of all (n = 25) dysplastic lesions exhibited coexpression of LIN28 and IL-6 and contained activated STAT3 (Figure 7G). These markers were hardly detected in normal liver or nontumor portion of HCV-infected livers.

DISCUSSION

The isolation and characterization of cells that can give rise to HCC only after transplantation into an appropriate host liver undergoing chronic injury demonstrates that cancer arises from progenitor cells that are yet to become fully malignant. Importantly, unlike fully malignant HCC cells, the HcPCs we isolated cannot form s.c. tumors or even liver tumors when introduced into a nondamaged liver. Liver damage induced by uPA expression or CCl_4 treatment provides HcPCs with the proper cytokine and growth factor milieu needed for their proliferation. Although HcPCs produce IL-6, they may also depend on other cytokines such as TNF, which is produced by macrophages that are recruited to the damaged liver. In addition, uPA expression and CCl_4 treatment may enhance HcPC growth and progression through their fibrogenic effect on hepatic stellate cells. Although HCC and other cancers have been suspected to arise from

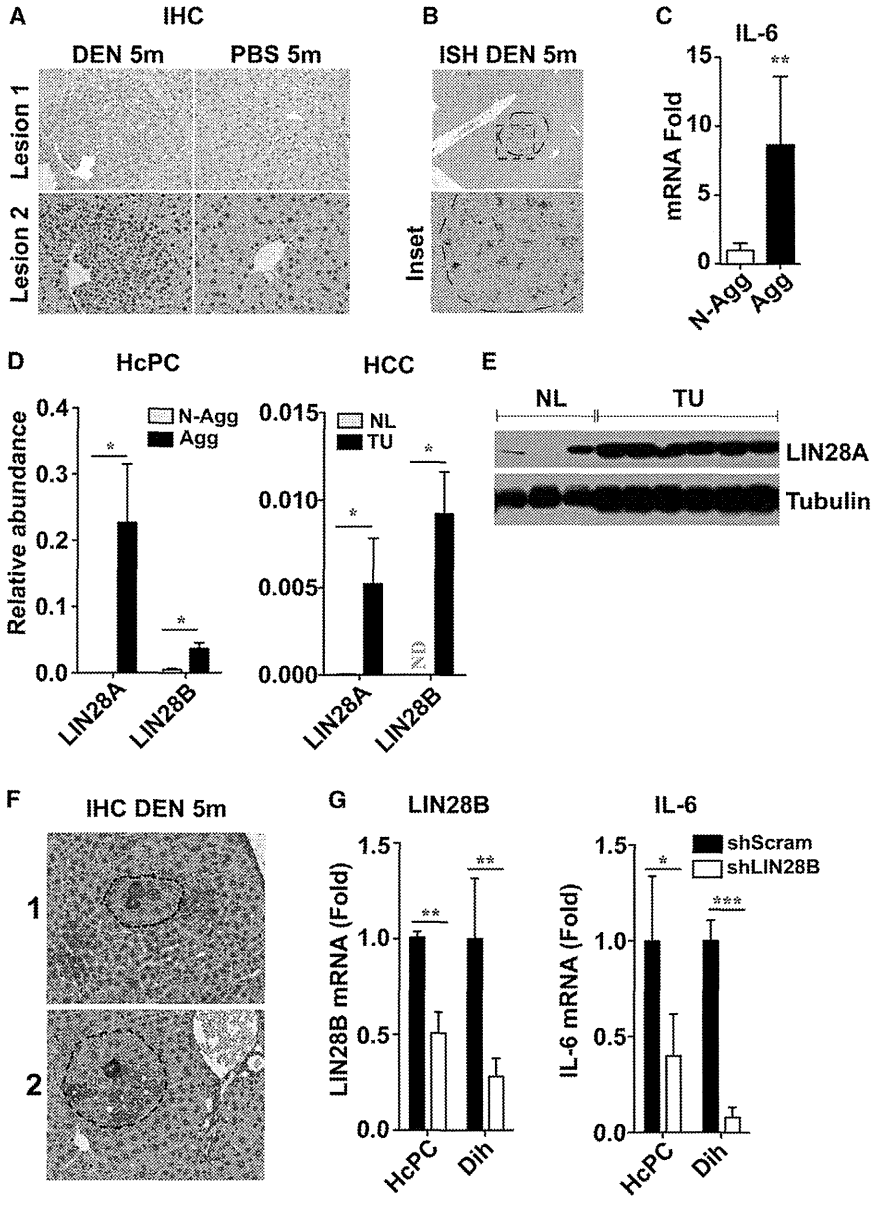

Figure 6. Liver Premalignant Lesions and HcPCs Exhibit Elevated IL-6 and LIN28 Expression

(A and B) Livers of 5-month-old DEN injected mice were analyzed for IL-6 expression by IHC (magnification: 400×) (A) and ISH (magnification: 100×, top; 400×, bottom) (B).

(C and D) Quantification of IL-6 (C) and LIN28 (D) mRNA in aggregated versus nonaggregated hepatocytes from 5-month-old DEN-treated livers and in normal versus tumor-bearing livers (n = 6; ± SEM) (ND, not detected).

(E) Immunoblot analyses of LIN28A in normal (NL) and tumor-bearing (TU) livers.

(F) DEN-treated livers were subjected to IHC with a LIN28A antibody. Broken lines indicate borders of FAH (400×).

(G) LIN28B was silenced with shRNA in HCC (dih) cells and cultured HcPCs, and LIN28B and IL-6 mRNAs were quantitated by qRT-PCR (n = 3; ± SEM).

See also Figure S5 and Table S2.

premalignant/dysplastic lesions (Hruban et al., 2007; Hytiroglou et al., 2007), a direct demonstration that such lesions progress into malignant tumors has been lacking. Based on expression of common markers—EpCAM, CD44, AFP, activated STAT3, and IL-6—that are not expressed in normal hepatocytes, we postulate that HcPCs originate from FAH or dysplastic foci, which are first observed in male mice within 3 months of DEN exposure. Indeed, the cells that are contained within the FAH are smaller than the surrounding parenchyma and are similar in size to isolated HcPCs. Importantly, FAH or premalignant dysplastic foci are not unique to DEN-treated rodents (Bannasch, 1984; Rabes, 1983), and similar lesions were detected in human cirrhotic livers (Hytiroglou et al., 2007; Seki et al., 2000; Takayama et al., 1990) in which the rate of HCC progression is 3%–5% per year (El-Serag, 2011). We found that human dysplastic lesions and mouse FAH and HcPC exhibit autocrine IL-6 signaling. HcPC are not unique to DEN-treated mice, and similar cells were isolated from *Tak1*$^{\Delta hep}$ mice in which HCC development resembles cirrhosis-associated human HCC (Inokuchi et al., 2010).

HcPC Origin and Relationship to Liver and HCC Stem Cells

Transcriptomic analysis indicates that DEN-induced HcPCs are related to both normal hepatobiliary bipotential stem cells/oval cells and HCC cells. Although HcPCs are not fully transformed, they express several markers—CD44, EpCAM, AFP, SOX9, OV6, and CK19—found to be expressed by HCC stem cells and oval cells (Guo et al., 2012; Mikhail and He, 2011; Terris et al., 2010; Yamashita et al., 2008; Zhu et al., 2010). However, unlike oval cells, which do not express albumin or AFP and do not give rise to liver tumors upon transplantation into MUP-uPA mice, HcPCs give rise to HCC after intrasplenic transplantation. Yet, unlike dih10 HCC cells, which express high levels of the HCC stem cell markers AFP, CD44, and EpCAM, HcPCs do not form s.c. tumors.

At this point, it is not clear whether HcPCs arise from oval cells or from dedifferentiated hepatocytes. Given that DEN is metabolically activated by Cyp2E1 that is expressed only in fully differentiated zone 3 hepatocytes (Tsutsumi et al., 1989) and that *Cyp2E1*$^{-/-}$ mice are refractory to DEN (Kang et al., 2007), DEN-induced HcPC are most likely derived from dedifferentiated hepatocytes. Consistent with this hypothesis, DEN-induced FAH and proliferating cells were found in zone 3 and not near bile ducts or the canals of Hering, sites at which oval cells reside

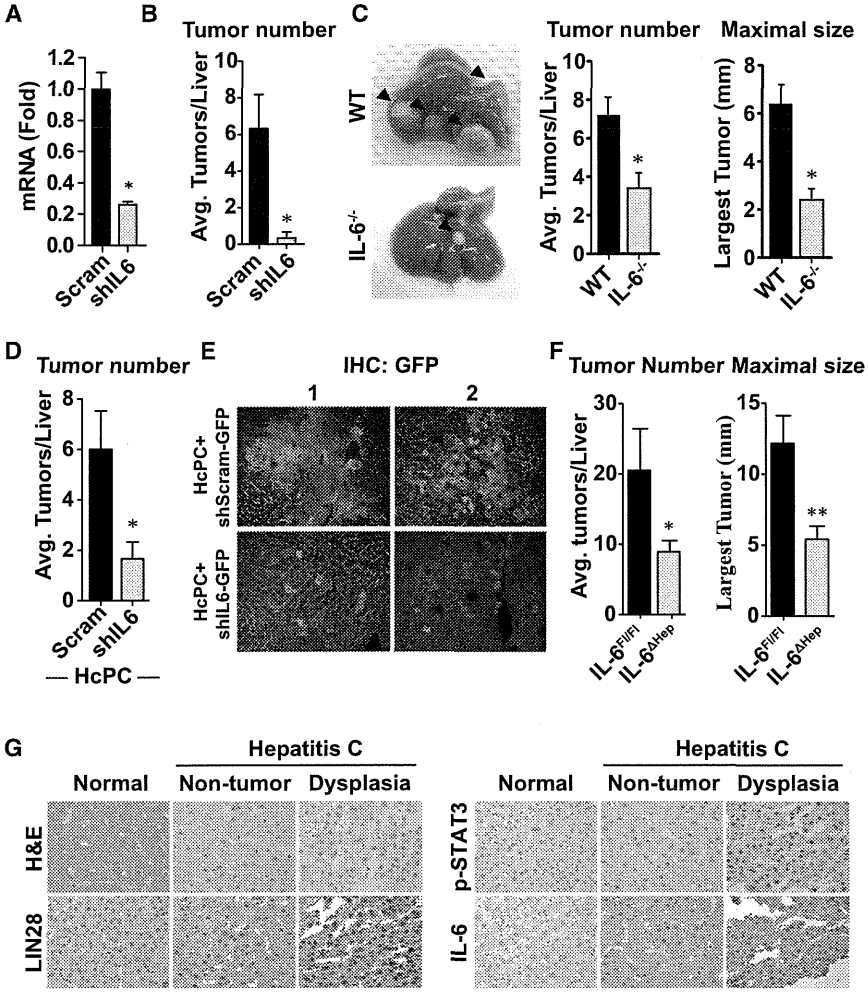

Figure 7. HCC Growth Depends on Autocrine IL-6 Production

(A) HCC cells (dih10) were transduced with lentiviruses containing scrambled or IL-6-specific shRNA. IL-6 mRNA was analyzed by qRT-PCR.

(B) Dih10 cells (1.2×10^5) transduced as above were i.s. injected into MUP-uPA mice that were analyzed 6 months later for HCC development (n = 3; ± SEM).

(C) HcPCs from WT and *Il6*$^{-/-}$ mice were injected (1×10^4 cells/mice) into MUP-uPA mice and analyzed 5 months later for HCC development (n = 5; ± SEM).

(D) HcPCs isolated from DEN-treated WT mice were transduced with shRNA against IL-6 or scrambled shRNA, cultured for 3 to 4 days, i.s. transplanted (1×10^4 cells/mice) into MUP-uPA mice, and analyzed 6 months later (n = 3; ± SEM).

(E) Livers of MUP-uPA mice from (D) were immunostained with GFP antibody 6 months after transplantation (200×). The bicistronic lentivirus in this experiment expresses GFP along with control or IL-6 shRNA, allowing tracking of the infected cells.

(F) DEN-treated *Il6*$^{\Delta hep}$ and *Il6*$^{F/F}$ mice were sacrificed after 9 months to evaluate tumor multiplicity and size (n = 6–10, ± SEM).

(G) IHC analysis of autocrine IL-6 signaling in human premalignant lesions in HCV-infected livers. Expression of LIN28, p-STAT3, and IL-6 was analyzed in 25 needle biopsies of dysplastic nodules, and representative positive specimens (n = 4) are shown. The dysplastic nodules and paired nontumor tissue were obtained from the same HCV-infected patient (n = 25). Nontumor tissue of metastatic liver cancer was used as normal control.

See also Figures S6 and S7.

(Duncan et al., 2009). Notably, GO analysis revealed that many of the genes whose expression is downregulated in HcPC-containing aggregates are involved in xenobiotic and organic acid metabolism, characteristics of differentiated hepatocytes. The same types of genes are also downregulated in HCC. However, final identification of the origin of HcPC will be provided by ongoing lineage-tracing experiments.

The Significance of Autocrine IL-6 Expression

Elevated IL-6 was detected in at least 40% of human HCCs, where it is expressed by the cancer cells (Soresi et al., 2006). More recent studies have confirmed upregulation of IL-6 in human HCC and suggested that it plays a central role in a gene expression network that drives tumor development (Ji et al., 2009). Elevated IL-6 was also found in viral and alcoholic hepatitis and liver cirrhosis, but in these conditions, IL-6 is expressed mainly by myeloid cells/leukocytes rather than parenchymal cells (Deviere et al., 1989; Kakumu et al., 1993; Soresi et al., 2006). Our studies indicate that the critical site of IL-6 expression shifts from myeloid cells to epithelial cells during the course of DEN-induced liver tumorigenesis. Initially, DEN administration rapidly induces IL-6 in Kupffer cells through NF-κB activation (Maeda et al., 2005). This initial surge in IL-6 is required for DEN-induced hepatocarcinogenesis (Naugler et al., 2007). Although IL-6 decays within 2 weeks of DEN administration, it reappears several months later, but at that time, it is expressed within FAH. IL-6 expression is also elevated in isolated HcPCs and is maintained in fully transformed HCC cells. Furthermore, autocrine IL-6 is important for HcPC to HCC progression and for tumorigenic growth. Autocrine IL-6 in both HcPC and HCC cells depends on elevated expression of LIN28, an RNA-binding protein that exerts its protumorigenic activity through downregulation of Let-7, an miRNA that inhibits IL-6 expression (Viswanathan and Daley, 2010). Accordingly, HcPCs exhibit downregulation of both Let-7f and Let-7g, and elevated LIN28 is found not only in isolated HcPCs but also within FAH and human HCV-induced dysplastic lesions.

A similar LIN28-Let-7-IL-6 epigenetic switch is important for in vitro programming and maintenance of cancer stem cells (Iliopoulos et al., 2009). IL-6 also induces malignant features in human ductal carcinoma stem cells (Sansone et al., 2007). In fact, autocrine IL-6 signaling was suggested to play a key role in STAT3-dependent tumor progression (Grivennikov and Karin, 2008). Another miRNA-driven autoregulatory circuit involved in

hepatocarcinogenesis accounts for elevated IL-6R expression (Hatziapostolou et al., 2011). Yet, HcPC-containing aggregates also express several other STAT3-activiting cytokines and receptors. Accordingly, silencing or ablation of IL-6 results in incomplete inhibition of HcPC to HCC progression. Nonetheless, our results demonstrate that autoregulatory circuits/epigenetic switches play an important role in the very early stages of tumorigenesis. Given that such circuits are already activated in premalignant cells, pharmacological agents that disrupt their function may be useful in cancer prevention. Prevention is of particular importance in cancers such as HCC, which is often detected at a stage that is refractory to currently available therapeutics.

EXPERIMENTAL PROCEDURES

Mice, HCC Induction, HcPC Isolation, and Transplantation

MUP-uPA transgenic mice (Weglarz et al., 2000) were maintained on a pure BL/6 background. Because homozygous females frequently die when pregnant, MUP-uPA heterozygotes were generated by backcrossing homozygous MUP-uPA males with BL/6 females to be used as recipients for hepatic transplantation. *Tak1*$^{\Delta hep}$ (Inokuchi et al., 2010) and *Il6*$^{F/F}$ (Quintana et al., 2013) mice were also in the BL/6 background. *Il6*$^{\Delta hep}$ mice were generated by crossing *Il6*$^{F/F}$ and *Alb-Cre* mice. C57BL/6 actin-GFP mice were from the Jackson Laboratories. BL/6 mice were purchased from Charles River Laboratories.

To induce HCC, 15-day-old mice were injected i.p. with 25 mg/kg DEN (Sigma). A pool of DEN-injected BL/6 mice was maintained and used in most experiments. Hepatocytes were isolated using a two-step procedure (He et al., 2010). Cell aggregates were isolated by filtration through 70 and 40 μm sieves. To disperse the aggregates into single cells, they were subjected to gentle pipetting in Ca/Mg-free PBS on ice. Single-cell suspensions of aggregated and nonaggregated hepatocytes were transplanted via an i.s. injection into 21-day-old male MUP-uPA mice (He et al., 2010). Alternatively, single-cell suspensions of aggregated hepatocytes were enriched for CD44^{+} HcPC using magnetic beads. As few as 100 viable CD44^{+} cells mixed with 1 × 10^{5} normal hepatocytes from normal males were transplanted into MUP-uPA mice. Alternatively, BL/6 mice were pretreated with retrorsine (70 mg/kg i.p.) (Sigma), a cell-cycle inhibitor, 1 month prior to transplantation. Transplanted mice were allowed to recover for 1 week and then injected weekly with 3× 0.5 ml/kg CCl_4 i.p. to induce liver injury and hepatocyte proliferation (Guo et al., 2002). Mice were sacrificed 5 to 6 months later, and tumors bigger than 1 mm in diameter on the liver surface were counted. Tumors bigger than 5 mm across were dissected for biochemical and molecular analyses.

ACCESSION NUMBERS

Raw gene expression array data have been deposited to NCBI's Gene Expression Omnibus under the GSE50431 study.

SUPPLEMENTAL INFORMATION

Supplemental Information includes Extended Experimental Procedures, seven figures, and three tables and can be found with this article online at http://dx.doi.org/10.1016/j.cell.2013.09.031.

AUTHOR CONTRIBUTIONS

G.H. identified, isolated, and characterized HcPCs; D.D. and H.N. optimized the HcPC isolation and purification procedure; D.D. found the mechanism of their dependence on autocrine IL-6 controlled by LIN28, characterized them using flow cytometry (with S.S.), and conducted miR analyses (with M.H. and D.I.); H.N. and D.D. used *Il6*$^{\Delta hep}$ mice to demonstrate in vivo HCC dependency on autocrine IL-6; H.N. (with R.T. and K.K.) found IL-6, LIN28, and P-STAT3 in human dysplastic lesions; J.F.-B. conducted the transcriptome analysis and exome sequencing (with S.E.Y., K.J., and O.H.) and with H.O. examined oncogenic potential of oval cells; H.O. examined HcPC proliferative potential and performed IF analysis of isolated HcPC (with A.S. and R.M.H.); Y.J. assisted with IHC and ISH staining; E.S. contributed to the experiments involving *Tak1*$^{\Delta hep}$ mice; G.H., D.D., J.F.-B., H.O., and M.K. wrote the manuscript.

ACKNOWLEDGMENTS

We acknowledge the Biogem facility at UCSD for their assistance with transcriptome analysis and A. Arian, K. Iwaisako, Y. Hiroshima, and H. Matsui for technical assistance. We thank Dr. J. Hidalgo (Universitat Autonoma de Barcelona, Spain) for the *Il6*$^{F/F}$ mice. Research was supported by the Superfund Basic Research Program (P42ES010337), NIH (CA118165 and CA155120), Wellcome Trust (WT086755), American Diabetes Association (7-08-MN-29), the Center for Translational Science (UL1RR031980 and UL1TR000100), the National Center for Research Resources IMAT program (N12R1CA155615), and postdoctoral research fellowships from the Damon Runyon Cancer Research Foundation (G.H.), American Liver Foundation (D.D.), Daiichi Sankyo Foundation of Life Science (H.N.), California Institute for Regenerative Medicine Stem Cell Training Grant II (TG2-01154) fellowship (J.F.-B.), Kanzawa Medical Research Foundation (H.O.), the German Research Foundation (DFG, SH721/1-1 to S.S.), and a Young Investigator Award from the National Childhood Cancer Foundation, "CureSearch" (D.D.). M.K. is an ACS Research Professor and is a recipient of the Ben and Wanda Hildyard Chair for Mitochondrial and Metabolic Diseases.

Received: December 11, 2012
Revised: June 4, 2013
Accepted: September 19, 2013
Published: October 10, 2013

REFERENCES

Bannasch, P. (1984). Sequential cellular changes during chemical carcinogenesis. J. Cancer Res. Clin. Oncol. *108*, 11–22.

Bladt, F., Riethmacher, D., Isenmann, S., Aguzzi, A., and Birchmeier, C. (1995). Essential role for the c-met receptor in the migration of myogenic precursor cells into the limb bud. Nature *376*, 768–771.

Deviere, J., Content, J., Denys, C., Vandenbussche, P., Schandene, L., Wybran, J., and Dupont, E. (1989). High interleukin-6 serum levels and increased production by leucocytes in alcoholic liver cirrhosis. Correlation with IgA serum levels and lymphokines production. Clin. Exp. Immunol. *77*, 221–225.

Dorrell, C., Erker, L., Schug, J., Kopp, J.L., Canaday, P.S., Fox, A.J., Smirnova, O., Duncan, A.W., Finegold, M.J., Sander, M., et al. (2011). Prospective isolation of a bipotential clonogenic liver progenitor cell in adult mice. Genes Dev. *25*, 1193–1203.

Duncan, A.W., Dorrell, C., and Grompe, M. (2009). Stem cells and liver regeneration. Gastroenterology *137*, 466–481.

Eferl, R., Ricci, R., Kenner, L., Zenz, R., David, J.P., Rath, M., and Wagner, E.F. (2003). Liver tumor development. c-Jun antagonizes the proapoptotic activity of p53. Cell *112*, 181–192.

El-Serag, H.B. (2011). Hepatocellular carcinoma. N. Engl. J. Med. *365*, 1118–1127.

Grivennikov, S., and Karin, M. (2008). Autocrine IL-6 signaling: a key event in tumorigenesis? Cancer Cell *13*, 7–9.

Guichard, C., Amaddeo, G., Imbeaud, S., Ladeiro, Y., Pelletier, L., Maad, I.B., Calderaro, J., Bioulac-Sage, P., Letexier, M., Degos, F., et al. (2012). Integrated analysis of somatic mutations and focal copy-number changes identifies key genes and pathways in hepatocellular carcinoma. Nat. Genet. *44*, 694–698.

Guo, D., Fu, T., Nelson, J.A., Superina, R.A., and Soriano, H.E. (2002). Liver repopulation after cell transplantation in mice treated with retrorsine and carbon tetrachloride. Transplantation *73*, 1818–1824.

Guo, X., Xiong, L., Sun, T., Peng, R., Zou, L., Zhu, H., Zhang, J., Li, H., and Zhao, J. (2012). Expression features of SOX9 associate with tumor progression and poor prognosis of hepatocellular carcinoma. Diagn. Pathol. *7*, 44.

Haridass, D., Yuan, Q., Becker, P.D., Cantz, T., Iken, M., Rothe, M., Narain, N., Bock, M., Nörder, M., Legrand, N., et al. (2009). Repopulation efficiencies of adult hepatocytes, fetal liver progenitor cells, and embryonic stem cell-derived hepatic cells in albumin-promoter-enhancer urokinase-type plasminogen activator mice. Am. J. Pathol. *175*, 1483–1492.

Hatziapostolou, M., Polytarchou, C., Aggelidou, E., Drakaki, A., Poultsides, G.A., Jaeger, S.A., Ogata, H., Karin, M., Struhl, K., Hadzopoulou-Cladaras, M., and Iliopoulos, D. (2011). An HNF4α-miRNA inflammatory feedback circuit regulates hepatocellular oncogenesis. Cell *147*, 1233–1247.

He, G., Yu, G.Y., Temkin, V., Ogata, H., Kuntzen, C., Sakurai, T., Sieghart, W., Peck-Radosavljevic, M., Leffert, H.L., and Karin, M. (2010). Hepatocyte IKKbeta/NF-kappaB inhibits tumor promotion and progression by preventing oxidative stress-driven STAT3 activation. Cancer Cell *17*, 286–297.

Hruban, R.H., Maitra, A., Kern, S.E., and Goggins, M. (2007). Precursors to pancreatic cancer. Gastroenterol. Clin. North Am. *36*, 831–849, vi.

Hytiroglou, P., Park, Y.N., Krinsky, G., and Theise, N.D. (2007). Hepatic precancerous lesions and small hepatocellular carcinoma. Gastroenterol. Clin. North Am. *36*, 867–887, vii.

Ichinohe, N., Kon, J., Sasaki, K., Nakamura, Y., Ooe, H., Tanimizu, N., and Mitaka, T. (2012). Growth ability and repopulation efficiency of transplanted hepatic stem cells, progenitor cells, and mature hepatocytes in retrorsine-treated rat livers. Cell Transplant. *21*, 11–22.

Iliopoulos, D., Hirsch, H.A., and Struhl, K. (2009). An epigenetic switch involving NF-kappaB, Lin28, Let-7 MicroRNA, and IL6 links inflammation to cell transformation. Cell *139*, 693–706.

Inokuchi, S., Aoyama, T., Miura, K., Osterreicher, C.H., Kodama, Y., Miyai, K., Akira, S., Brenner, D.A., and Seki, E. (2010). Disruption of TAK1 in hepatocytes causes hepatic injury, inflammation, fibrosis, and carcinogenesis. Proc. Natl. Acad. Sci. USA *107*, 844–849.

Ji, J., Shi, J., Budhu, A., Yu, Z., Forgues, M., Roessler, S., Ambs, S., Chen, Y., Meltzer, P.S., Croce, C.M., et al. (2009). MicroRNA expression, survival, and response to interferon in liver cancer. N. Engl. J. Med. *361*, 1437–1447.

Kakumu, S., Shinagawa, T., Ishikawa, T., Yoshioka, K., Wakita, T., and Ida, N. (1993). Interleukin 6 production by peripheral blood mononuclear cells in patients with chronic hepatitis B virus infection and primary biliary cirrhosis. Gastroenterol. Jpn. *28*, 18–24.

Kang, J.S., Wanibuchi, H., Morimura, K., Gonzalez, F.J., and Fukushima, S. (2007). Role of CYP2E1 in diethylnitrosamine-induced hepatocarcinogenesis in vivo. Cancer Res. *67*, 11141–11146.

Laconi, E., Oren, R., Mukhopadhyay, D.K., Hurston, E., Laconi, S., Pani, P., Dabeva, M.D., and Shafritz, D.A. (1998). Long-term, near-total liver replacement by transplantation of isolated hepatocytes in rats treated with retrorsine. Am. J. Pathol. *153*, 319–329.

Maeda, S., Kamata, H., Luo, J.L., Leffert, H., and Karin, M. (2005). IKKbeta couples hepatocyte death to cytokine-driven compensatory proliferation that promotes chemical hepatocarcinogenesis. Cell *121*, 977–990.

Marquardt, J.U., and Thorgeirsson, S.S. (2010). Stem cells in hepatocarcinogenesis: evidence from genomic data. Semin. Liver Dis. *30*, 26–34.

Meyer, K., Lee, J.S., Dyck, P.A., Cao, W.Q., Rao, M.S., Thorgeirsson, S.S., and Reddy, J.K. (2003). Molecular profiling of hepatocellular carcinomas developing spontaneously in acyl-CoA oxidase deficient mice: comparison with liver tumors induced in wild-type mice by a peroxisome proliferator and a genotoxic carcinogen. Carcinogenesis *24*, 975–984.

Mikhail, S., and He, A.R. (2011). Liver cancer stem cells. Int. J. Hepatol. *2011*, 486954.

Naugler, W.E., Sakurai, T., Kim, S., Maeda, S., Kim, K., Elsharkawy, A.M., and Karin, M. (2007). Gender disparity in liver cancer due to sex differences in MyD88-dependent IL-6 production. Science *317*, 121–124.

Nguyen, L.V., Vanner, R., Dirks, P., and Eaves, C.J. (2012). Cancer stem cells: an evolving concept. Nat. Rev. Cancer *12*, 133–143.

Nowell, P.C. (1976). The clonal evolution of tumor cell populations. Science *194*, 23–28.

Park, E.J., Lee, J.H., Yu, G.Y., He, G., Ali, S.R., Holzer, R.G., Osterreicher, C.H., Takahashi, H., and Karin, M. (2010). Dietary and genetic obesity promote liver inflammation and tumorigenesis by enhancing IL-6 and TNF expression. Cell *140*, 197–208.

Pitot, H.C. (1990). Altered hepatic foci: their role in murine hepatocarcinogenesis. Annu. Rev. Pharmacol. Toxicol. *30*, 465–500.

Porta, C., De Amici, M., Quaglini, S., Paglino, C., Tagliani, F., Boncimino, A., Moratti, R., and Corazza, G.R. (2008). Circulating interleukin-6 as a tumor marker for hepatocellular carcinoma. Ann. Oncol. *19*, 353–358.

Quintana, A., Erta, M., Ferrer, B., Comes, G., Giralt, M., and Hidalgo, J. (2013). Astrocyte-specific deficiency of interleukin-6 and its receptor reveal specific roles in survival, body weight and behavior. Brain Behav. Immun. *27*, 162–173.

Rabes, H.M. (1983). Development and growth of early preneoplastic lesions induced in the liver by chemical carcinogens. J. Cancer Res. Clin. Oncol. *106*, 85–92.

Rhim, J.A., Sandgren, E.P., Degen, J.L., Palmiter, R.D., and Brinster, R.L. (1994). Replacement of diseased mouse liver by hepatic cell transplantation. Science *263*, 1149–1152.

Sansone, P., Storci, G., Tavolari, S., Guarnieri, T., Giovannini, C., Taffurelli, M., Ceccarelli, C., Santini, D., Paterini, P., Marcu, K.B., et al. (2007). IL-6 triggers malignant features in mammospheres from human ductal breast carcinoma and normal mammary gland. J. Clin. Invest. *117*, 3988–4002.

Seki, S., Sakaguchi, H., Kitada, T., Tamori, A., Takeda, T., Kawada, N., Habu, D., Nakatani, K., Nishiguchi, S., and Shiomi, S. (2000). Outcomes of dysplastic nodules in human cirrhotic liver: a clinicopathological study. Clin. Cancer Res. *6*, 3469–3473.

Sell, S., and Leffert, H.L. (2008). Liver cancer stem cells. J. Clin. Oncol. *26*, 2800–2805.

Shin, S., Walton, G., Aoki, R., Brondell, K., Schug, J., Fox, A., Smirnova, O., Dorrell, C., Erker, L., Chu, A.S., et al. (2011). Foxl1-Cre-marked adult hepatic progenitors have clonogenic and bilineage differentiation potential. Genes Dev. *25*, 1185–1192.

Soresi, M., Giannitrapani, L., D'Antona, F., Florena, A.M., La Spada, E., Terranova, A., Cervello, M., D'Alessandro, N., and Montalto, G. (2006). Interleukin-6 and its soluble receptor in patients with liver cirrhosis and hepatocellular carcinoma. World J. Gastroenterol. *12*, 2563–2568.

Su, Y., Kanamoto, R., Miller, D.A., Ogawa, H., and Pitot, H.C. (1990). Regulation of the expression of the serine dehydratase gene in the kidney and liver of the rat. Biochem. Biophys. Res. Commun. *170*, 892–899.

Su, Q., Benner, A., Hofmann, W.J., Otto, G., Pichlmayr, R., and Bannasch, P. (1997). Human hepatic preneoplasia: phenotypes and proliferation kinetics of foci and nodules of altered hepatocytes and their relationship to liver cell dysplasia. Virchows Arch. *431*, 391–406.

Takayama, T., Makuuchi, M., Hirohashi, S., Sakamoto, M., Okazaki, N., Takayasu, K., Kosuge, T., Motoo, Y., Yamazaki, S., and Hasegawa, H. (1990). Malignant transformation of adenomatous hyperplasia to hepatocellular carcinoma. Lancet *336*, 1150–1153.

Terris, B., Cavard, C., and Perret, C. (2010). EpCAM, a new marker for cancer stem cells in hepatocellular carcinoma. J. Hepatol. *52*, 280–281.

Tsutsumi, M., Lasker, J.M., Shimizu, M., Rosman, A.S., and Lieber, C.S. (1989). The intralobular distribution of ethanol-inducible P450IIE1 in rat and human liver. Hepatology *10*, 437–446.

Verna, L., Whysner, J., and Williams, G.M. (1996). N-nitrosodiethylamine mechanistic data and risk assessment: bioactivation, DNA-adduct formation, mutagenicity, and tumor initiation. Pharmacol. Ther. *71*, 57–81.

Viswanathan, S.R., and Daley, G.Q. (2010). Lin28: A microRNA regulator with a macro role. Cell *140*, 445–449.

Wang, R., Ferrell, L.D., Faouzi, S., Maher, J.J., and Bishop, J.M. (2001). Activation of the Met receptor by cell attachment induces and sustains hepatocellular carcinomas in transgenic mice. J. Cell Biol. *153*, 1023–1034.

Weglarz, T.C., Degen, J.L., and Sandgren, E.P. (2000). Hepatocyte transplantation into diseased mouse liver. Kinetics of parenchymal repopulation and identification of the proliferative capacity of tetraploid and octaploid hepatocytes. Am. J. Pathol. *157*, 1963–1974.

Wood, L.D., Parsons, D.W., Jones, S., Lin, J., Sjöblom, T., Leary, R.J., Shen, D., Boca, S.M., Barber, T., Ptak, J., et al. (2007). The genomic landscapes of human breast and colorectal cancers. Science *318*, 1108–1113.

Yamashita, T., Forgues, M., Wang, W., Kim, J.W., Ye, Q., Jia, H., Budhu, A., Zanetti, K.A., Chen, Y., Qin, L.X., et al. (2008). EpCAM and alpha-fetoprotein expression defines novel prognostic subtypes of hepatocellular carcinoma. Cancer Res. *68*, 1451–1461.

Yang, Z.F., Ho, D.W., Ng, M.N., Lau, C.K., Yu, W.C., Ngai, P., Chu, P.W., Lam, C.T., Poon, R.T., and Fan, S.T. (2008). Significance of CD90+ cancer stem cells in human liver cancer. Cancer Cell *13*, 153–166.

Zheng, T., Wang, J., Jiang, H., and Liu, L. (2011). Hippo signaling in oval cells and hepatocarcinogenesis. Cancer Lett. *28*, 91–99.

Zhu, Z., Hao, X., Yan, M., Yao, M., Ge, C., Gu, J., and Li, J. (2010). Cancer stem/progenitor cells are highly enriched in CD133+CD44+ population in hepatocellular carcinoma. Int. J. Cancer *126*, 2067–2078.

Zöller, M. (2009). Tetraspanins: push and pull in suppressing and promoting metastasis. Nat. Rev. Cancer *9*, 40–55.

PLOS | ONE

Identification of a Functional Variant in the *MICA* Promoter Which Regulates *MICA* Expression and Increases HCV-Related Hepatocellular Carcinoma Risk

Paulisally Hau Yi Lo[1], Yuji Urabe[1,2], Vinod Kumar[1], Chizu Tanikawa[1], Kazuhiko Koike[3], Naoya Kato[4], Daiki Miki[2,5], Kazuaki Chayama[2,5], Michiaki Kubo[5], Yusuke Nakamura[1,6], Koichi Matsuda[1]*

1 Laboratory of Molecular Medicine, Human Genome Center, Institute of Medical Science, The University of Tokyo, Tokyo, Japan, **2** Departments of Medical and Molecular Science, Division of Frontier Medical Science, Programs for Biomedical Research, Graduate School of Biomedical Sciences, Hiroshima University, Hiroshima, Japan, **3** Department of Gastroenterology, Graduate School of Medicine, University of Tokyo, Tokyo, Japan, **4** Unit of Disease Control Genome Medicine, The Institute of Medical Science, The University of Tokyo, Tokyo, Japan, **5** Center for Genomic Medicine, The Institute of Physical and Chemical Research (RIKEN), Kanagawa, Japan, **6** Departments of Medicine and Surgery, and Center for Personalized Therapeutics, The University of Chicago, Chicago, Illinois, United States of America

Abstract

Hepatitis C virus (HCV) infection is the major cause of hepatocellular carcinoma (HCC) in Japan. We previously identified the association of SNP rs2596542 in the 5′ flanking region of the *MHC class I polypeptide-related sequence A* (*MICA*) gene with the risk of HCV-induced HCC. In the current study, we performed detailed functional analysis of 12 candidate SNPs in the promoter region and found that a SNP rs2596538 located at 2.8 kb upstream of the *MICA* gene affected the binding of a nuclear protein(s) to the genomic segment including this SNP. By electrophoretic mobility shift assay (EMSA) and chromatin immunoprecipitation (ChIP) assay, we identified that transcription factor Specificity Protein 1 (SP1) can bind to the protective G allele, but not to the risk A allele. In addition, reporter construct containing the G allele was found to exhibit higher transcriptional activity than that containing the A allele. Moreover, SNP rs2596538 showed stronger association with HCV-induced HCC ($P = 1.82 \times 10^{-5}$ and OR = 1.34) than the previously identified SNP rs2596542. We also found significantly higher serum level of soluble MICA (sMICA) in HCV-induced HCC patients carrying the G allele than those carrying the A allele ($P = 0.00616$). In summary, we have identified a functional SNP that is associated with the expression of MICA and the risk for HCV-induced HCC.

Citation: Lo PHY, Urabe Y, Kumar V, Tanikawa C, Koike K, et al. (2013) Identification of a Functional Variant in the *MICA* Promoter Which Regulates *MICA* Expression and Increases HCV-Related Hepatocellular Carcinoma Risk. PLoS ONE 8(4): e61279. doi:10.1371/journal.pone.0061279

Editor: Erica Villa, University of Modena & Reggio Emilia, Italy

Received September 24, 2012; **Accepted** March 11, 2013; **Published** April 11, 2013

Funding: This work was supported by the Ministry of Education, Culture, Sports, Science and Technology of the Japanese government, the Ministry of Health, Labour, and Welfare of the Japanese government. The funders had no role in study design, data collection and analysis, decision to publish, or preparation of the manuscript.

Competing Interests: The authors have declared that no competing interests exist.

* E-mail: koichima@ims.u-tokyo.ac.jp

Introduction

Hepatocellular carcinoma (HCC) is one of the common cancers in the world. It is well-known to be associated with the chronic infection of Hepatitis B (HBV) and Hepatitis C (HCV) viruses. In Japan, nearly 70% of HCC patients are infected with HCV [1]. The annual rate of developing HCC among patients with HCV-related liver cirrhosis in Japan is estimated to be about 4–8 percent [2]. Recent analyses have identified various genetic factors that are related with viral induced liver diseases [3–5]. In our previous two-stage genome-wide association study (GWAS) using a total number of 1,394 cases and 5,486 controls, a SNP rs2596542 located on chromosome 6p21.33 was shown to be significantly associated with HCV-induced HCC ($P = 4.21 \times 10^{-13}$ and OR = 1.39) [6]. This SNP is located within the class I major histocompatibility complex (MHC) region and is at about 4.8 kb upstream of *MHC class I polypeptide-related sequence A* (*MICA*) gene. We also identified that the risk A allele of SNP rs2596542 was strongly associated with the low expression of soluble MICA (sMICA) in the serum of HCV-related HCC patients [6].

MICA is a membrane protein which is up-regulated in various tumor cells and also induced in response to various cellular stresses such as infection, hypoxia, and heat shock [7]. It is an important component of the innate immune response, as MICA can bind to the NKG2D receptor and subsequently activate natural killer (NK) cells, CD8+ cells, and γδ T cells [8,9]. Moreover, membrane MICA can be shed by metalloproteinases, including MMP9, ADAM10, and ADAM17, and secreted into serum as a soluble form [10,11]. Since these metalloproteinases are often activated in HCC, the expressions of both membrane-bound MICA and sMICA are increased [12,13]. SNP rs2596542 was found to be associated with the progression from chronic hepatitis C (CHC) to HCC and also with serum sMICA level. Hence, both rs2596542 and sMICA would be possible prognostic biomarkers for CHC patients. However, their underlying molecular mechanisms were not fully elucidated so far.

We hypothesize that *MICA* variations could affect sMICA level by either one or both of the following two possible mechanisms: (1) the genetic variation(s) in the coding region affecting the protein stability and (2) the transcriptional regulation. Previously, variable

numbers of tandem repeats (VNTRs) in exon 5 of *MICA* were identified to affect MICA subcellular localization and serum MICA level [14]. The exon 5 of *MICA* encodes the transmembrane domain and the insertion of an extra G nucleotide in the domain would result in a premature stop codon that would generate MICA protein without a transmembrane domain and subsequently affect sMICA level [14]. However, our previous results indicated that MICA VNTR was not significantly associated with the sMICA level or HCC risk [6]. Therefore, in the current study, we have tried to investigate whether the *MICA* variations would affect the *MICA* transcription in the liver cancer cells. Through the functional analysis of genetic variations in the *MICA* promoter region, we here report a causative SNP rs2596538 that increases the binding affinity of the transcription factor Specificity Protein 1 (SP1) and the risk of progression of the disease.

Materials and Methods

Samples and genotyping

DNA samples for direct sequencing (50 HCV-related HCC cases), imputation analysis (721 HCV-related HCC cases and 5,486 HCV-negative controls), and serum samples for sMICA ELISA (246 HCV-related HCC) were obtained from BioBank Japan [15,16]. Genotyping of SNPs from 1,394 HCC patients and measurement of sMICA expression by ELISA were performed in the previous study [6]. Genotyping of SNP rs2596542 in 1,043 CHC was performed previously in RIKEN using Illumina HumanHap610-Quad BeadChip [17]. All CHC subjects had abnormal levels of serum alanine transaminase for more than 6 months and were positive for both HCV antibody and serum HCV RNA. The SNP rs2596542 in liver cirrhosis samples without hepatocellular carcinoma from BioBank Japan (n = 420) and the University of Tokyo (n = 166) were genotyped using Illumina HumanHap610-Quad BeadChip or invader assay [18]. All subjects were either subjected to liver biopsy or diagnosed by non-invasive methods including hepatic imaging, biochemical data, and the presence/absence of clinical manifestations of portal hypertension [18]. The samples used in the current project were listed in Table S1. Case samples with HBV co-infection were excluded from this study. The subjects with cancers, chronic hepatitis B, diabetes or tuberculosis were excluded from non-HCV controls. All subjects were Japanese origin and provided written informed consent. This research project was approved by the ethical committees of the University of Tokyo and RIKEN.

Imputation study

The imputation study was performed by using a hidden Markov model programmed in MACH [19] and haplotype information from 1000 genomes database [20]. The imputation results were confirmed by direct DNA sequencing in 50 randomly selected samples.

Cell culture

Human liver cancer cell lines HLE and HepG2 were purchased from JHSF (Osaka, Japan) and ATCC. These cells were grown in Dulbecco's modified Eagle's medium (Invitrogen) with 10% fetal bovine serum. Cells were cultured at 37°C with 5% CO_2.

EMSA

HLE cells were grown in 15 cm culture plate until they reached 95% confluency. The plate was then sealed with parafilm and immersed in a water bath at 42.5°C for 1.5 hours [21]. Nuclear extracts from these cells were prepared according to the standard protocol [22]. EMSA was carried out using DIG Gel Shift Kit, 2nd Generation (Roche) according to the manufacturer's instructions. The sequences of the 12 probes were listed in the Table S2. In brief, 30 fmol of labeled probes were hybridized with 5 μg nuclear extract for 15 minutes at room temperature. The mixtures were then loaded into a 6% TBE gel, separated by electrophoresis at 4°C and transferred onto a nylon membrane. The membrane was then hybridized with anti-digoxigenin-AP antibody and developed by CSPD solution. For competition study, nuclear extracts were incubated with non-labeled oligonucleotides first before adding labeled probe. For supershift assay, SP1 antibody (SC-59X, Santa Cruz Biotechnology) was added into the nuclear extract and incubated on ice for 30 minutes first before adding labeled probe. The mixtures were then separated by electrophoresis using 4% TBE gel. All EMSAs were repeated twice for reconfirmation of the results.

ChIP

The HLE cells (G allele homozygote) and HepG2 cells (heterozygote) were used in the ChIP assay. The plasmid pCAGGS-SP1 was transfected into both cells by using FuGENE6 Transfection Reagent (Roche). The ChIP assays were carried out using Chromatin Immunoprecipitation Assay Kit (Millipore) according to the manufacturer's protocol. In brief, the cells were treated with formaldehyde to crosslink DNA-protein complexes at 48 hours post-transfection. DNA-protein complexes were then sheared by sonication and immunoprecipitated by rabbit polyclonal anti-SP1 antibody (SC-59X, Santa Cruz Biotechnology). The resulting DNAs were analyzed by PCR (Table S2). In order to determine the binding specificity of SP1 to the SNP rs2596538 allele, the PCR products from HepG2 cells were further subcloned into pCR 2.1 vector and sequenced to assess G to A ratio in both input DNA and immunoprecipitant.

Dual luciferase reporter assay

Three copies of 31 bp DNA fragments equivalent to the EMSA oligonucleotides of SNP rs2596538 were cloned into pGL3-promoter vector (Promega). The plasmids were co-transfected with pCAGGS-SP1 and pRL-TK plasmids (Promega) into HLE cells by FuGENE6 Transfection Reagent (Roche). The pCAGGS-SP1 plasmid provided the expression of transcription factor SP1, and pRL-TK plasmid served as internal control for transfection efficiency [23]. The cells were lysed at 48 hours post-transfection, and relative luciferase activities were measured by Dual Luciferase Assay System (Toyo B-Net).

Western blotting

Cancer cell lysates were prepared by using pre-chilled RIPA buffer, and 25 μg of each lysate was loaded into the gel and separated by SDS-PAGE. Western blotting was performed according to the standard protocol. Rabbit anti-MICA antibody (ab63709, abcam: 1/1000) and rabbit anti-SP1 antibody (17-601, Upstate Biotechnology: 1/500) were used in the experiment.

Statistical analysis

The case-control association was analyzed by Student's *t*-test and Fisher's exact test as appropriate. The association of allele dependent sMICA expression was studied by Kruskal-Wallis test using R statistical environment version 2.8.1. The LD and coefficients (D' and r^2) were calculated by Haploview version 4.2 [24].

Table 1. Association of rs2596542 with the progression from CHC to LC and HCC.

	Case MAF	Control MAF	P^*	OR	95% C.I.
LC vs CHC	0.3797	0.3442	0.04842	1.166	1.01–1.35
HCC vs LC	0.4012	0.3797	0.20296	1.094	0.95–1.26

MAF, minor allele frequency; OR, odds ratio for minor allele. C.I., confidence interval. SNP rs2596542 was analyzed in 1,043 chronic hepatitis C (CHC), 586 liver cirrhosis without hepatocellular carcinoma (LC) and 1,394 HCV-induce hepaticellular carcinoma patients (HCC). *calculated by Armitage trend test.
doi:10.1371/journal.pone.0061279.t001

Results

Analyses of SNP rs2596542 in HCV-infected patients at different disease stages

Since the development of HCC consists of multiple steps, we investigated the role of SNP rs2596542 with disease progression. SNP rs2596542 was genotyped in patients at three different disease categories of CHC (chronic hepatitis C) without liver cirrhosis (LC) or HCC, LC without HCC, and HCC. The statistical analysis indicated that SNP rs2596542 was significantly associated with disease progression from CHC to LC with P-value of 0.048 and odds ratio of 1.17 (Table 1). The risk allele frequency among HCC patients (40.1%) was higher than that among LC patients (38.0%), but the association was not statistically significant (P-value of 0.203 and odds ratio of 1.09). These results suggested the involvement of *MICA* with both liver fibrosis and hepatocellular carcinogenesis.

HCV-HCC risk is not associated with MICA copy number variation

A previous report has indicated the deletion of the entire *MICA* locus in 3.2% of Japanese population [25] and this deletion was shown to be associated with the risk of nasopharyngeal carcinoma (NPC), especially in male [26]. To identify the functional SNP that may affect *MICA* mRNA expression, we analyzed the relation between the *MICA* copy number variation (CNV) and the HCC susceptibility. We quantified this CNV by real-time PCR in 375 HCV-related HCC patients and 350 HCV-negative controls. As shown in Table S3, we found no difference in the copy numbers between HCC cases and controls, indicating that this CNV is unlikely to be causative genetic variation for the risk of HCC.

Direct sequencing of 5′ flanking region of *MICA*

We then focused on the variations in the 5' flanking region of the *MICA* gene which may be associated with its promoter activity. We had conducted direct DNA sequencing of the 5-kb promoter region which included the marker SNP rs2596542 using genomic DNAs of 50 HCC subjects and identified 11 SNPs showing strong linkage disequilibrium with the marker SNP rs2596542 ($D'>0.953$ and $r^2>0.832$) (Fig. S1, Table 2).

Allele specific binding of nuclear protein to genomic region including SNP rs2596538

To investigate whether these genetic variations would affect the binding affinity of some transcription factors, we had conducted the electrophoretic mobility shift assay (EMSA) using the nuclear extract of HLE human hepatocellular carcinoma cells. Since MICA is a stress-inducible protein [21], we first treated the cells with heat shock treatment at 42°C for 90 minutes and confirmed significant induction of MICA expression as shown in Fig. 1a. Then we performed EMSA using 24 labeled-oligonucleotides corresponding to each allele of the 12 candidates' SNPs. The results of EMSA demonstrated that an oligonucleotide corresponding to a G allele of SNP rs2596538 exhibited stronger binding affinity to a nuclear protein(s) than that to an A allele (Fig. 1b). We then confirmed the specific binding of nuclear proteins to the G allele by competitor assay using non-labeled oligonucleotides (Fig. 1c). The self (G allele) oligonucleotides inhibited the formation of DNA-protein complex in a dose-dependent manner, but the non-self (A allele) oligonucleotides showed no inhibition effect. Taken together, some nuclear protein(s) in hepatocellular carcinoma cells would interact with a DNA fragment including the G allele of SNP rs2596538.

Table 2. Linkage disequilibrium between 11 candidate SNPs and SNP rs2596542.

SNP ID	Relative position[a]	A1	A1 frequency	D'	r^2
rs2596542	−4815	A	0.36		
rs2428475	−4788	G	0.36	1	1
rs28366144	−4586	T	0.36	1	1
rs2428474	−4387	G	0.39	1	0.88
rs2251731	−4045	A	0.39	1	0.88
rs2844526	−3703	C	0.38	1	0.918
rs2596541	−3572	A	0.38	1	0.918
rs2523453	−3285	G	0.38	1	0.918
rs2544525	−3259	C	0.38	1	0.918
rs2523452	−2870	G	0.34	0.953	0.832
rs2596538	−2778	A	0.34	0.953	0.832
rs2844522	−2710	C	0.34	0.953	0.832

Note: Direct DNA sequence of 5-kb promoter region of MICA from 50 HCV-HCC subjects. D' and r^2 were calculated by comparing the genotypes of these SNPs to the marker SNP rs2596542 by Haploview. A1, minor allele; [a]Relative position to exon 1 of the *MICA* gene.
doi:10.1371/journal.pone.0061279.t002

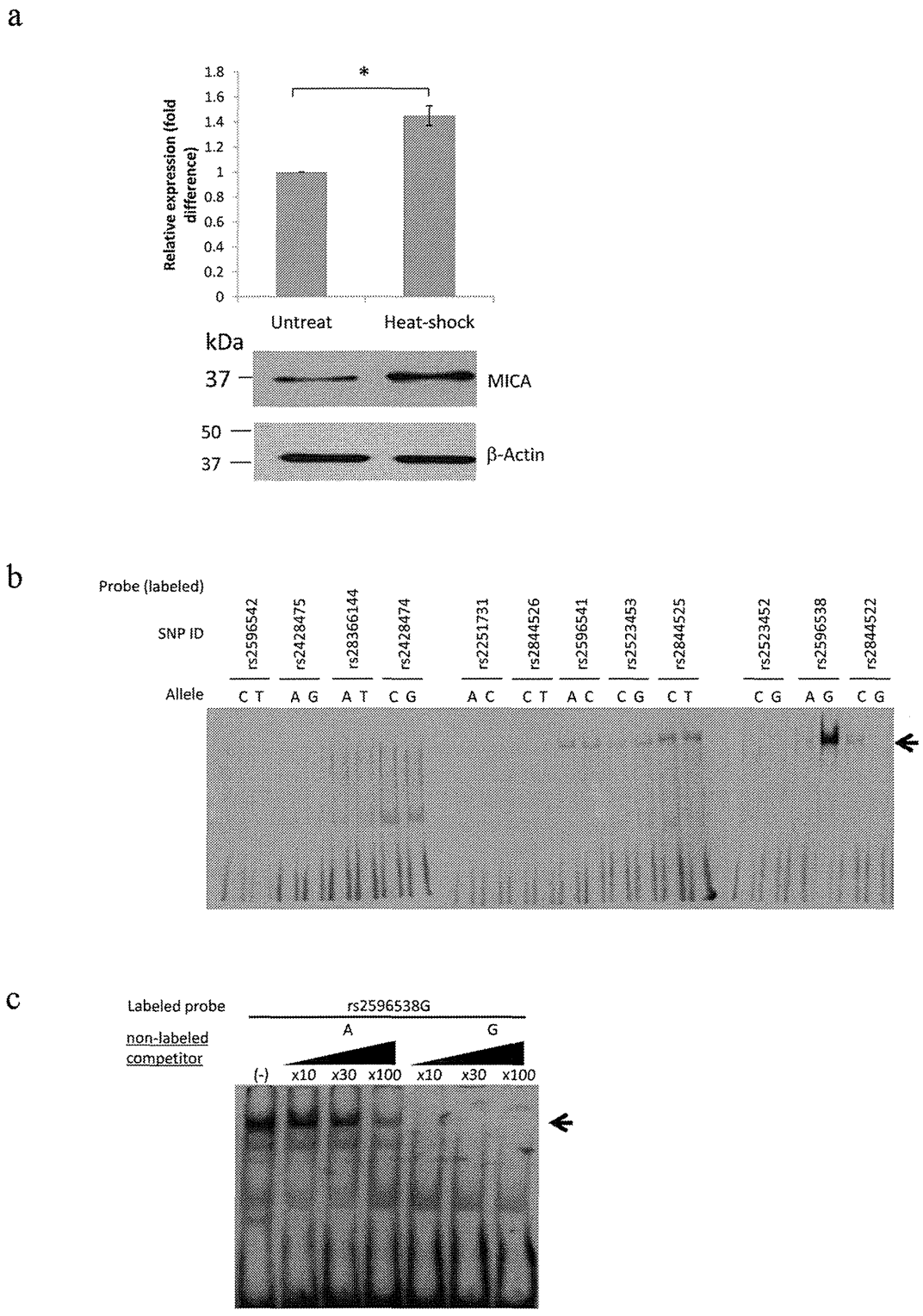

Figure 1. SNP rs2596538 affects the binding affinity of nuclear proteins. (**A**) Real-time quantitative PCR (upper) and Western blotting (lower) of MICA before and after heat shock treatment in HLE cells. *B2M* and β-actin are served as internal and protein loading control. (**B**) EMSA using 31 bp labeled probes flanking each SNP located within the 4.8 kb region upstream of *MICA* transcription start site. A black arrow indicates the shifted band specific to G allele of SNP rs2596538. (**C**) EMSA using the labeled G allele of SNP rs2596538 and nuclear extract from heat treated HLE cells. Non-labeled A or G allele of SNP rs2596538 at different concentrations are used as competitors. Pointed arrow indicates shifted band. *$P<0.05$ by Student's *t*-test.

doi:10.1371/journal.pone.0061279.g001

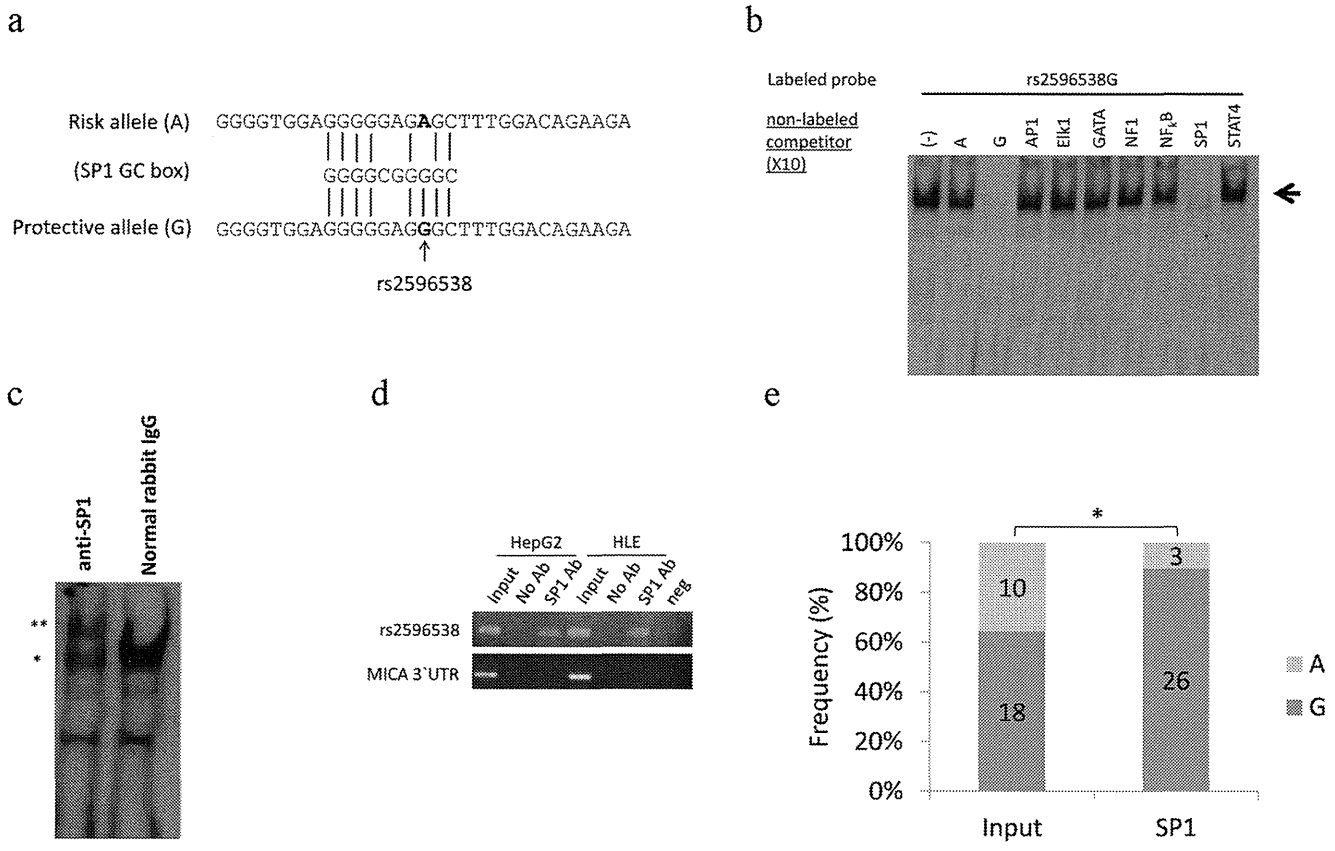

Figure 2. Binding of transcription factor SP1 to G allele of SNP rs2596538. (**A**) Multiple alignment of a GC box and DNA sequence of A or G probe of SNP rs2596538 used in EMSA. (**B**) EMSA using the labeled G allele of SNP rs2596538 and nuclear extract from heat treated HLE cells. Non-labeled consensus oligonucleotides of seven transcription factors are used as competitors. Pointed arrow indicates shifted band. (**C**) EMSA using the labeled G allele of SNP rs2596538 and nuclear extract from heat shock treated HLE cells in the presence of anti-SP1 antibody or normal rabbit IgG. Asterisks on the left side indicate the shifted (*) and super-shifted bands (**). Normal rabbit IgG serves as a negative control. (**D**) ChIP assay using HepG2 and HLE cell lines were ectopically expressed with SP1 protein. DNA-protein complex was immunoprecipitated with anti-SP1 antibody followed by PCR amplification using a primer pair flanking SNP rs2596538. DNAs precipitated without antibody are served as a negative control. PCR primers flanking the 3′ UTR region of *MICA* are served as a negative control. (**E**) Genotype distribution at SNP rs2596538 in PCR fragment amplified from the input genomic DNA and DNA-protein complex immunopurified from HepG2 cells by using anit-SP1 antibody. *$P<0.05$ by Student's *t*-test.
doi:10.1371/journal.pone.0061279.g002

SNP rs2596538 regulates the binding of SP1

Since *in silico* analysis identified a putative GC box in a protective G allele but not in a risk A allele (Fig. 2a), the transcription factor SP1 might preferentially bind to the G allele. Base on this information, we further performed competitor assay using non-labeled oligonucleotides (Table S2) and found that among seven tested oligonucleotides, only SP1-consensus oligonucleotides could effectively inhibit the binding of the nuclear protein(s) to the labeled G allele (Fig. 2b). In addition, we identified that the addition of anti-SP1 antibody caused a supershift of a band corresponding to the DNA-protein complex while control IgG did not cause the band shift (Fig. 2c). This result clearly indicated that the SP1 protein is very likely to be a component of the DNA-protein complex.

Furthermore, we performed chromatin immunoprecipitation (ChIP) assay to confirm the binding of SP1 to this genomic region *in vivo*. We had used two cell lines with different genetic backgrounds at SNP rs2596538 locus: HLE cells carrying the only G allele, while HepG2 cells harboring both A and G alleles. After the introduction of SP1 expression vector (pCAGGS-SP1) into these cell lines, the cell extracts were subjected to ChIP assay using anti-SP1 antibody (Fig. 2d). Subsequent PCR experiments indicated that SP1 bound to a genomic fragment containing the G allele of SNP rs2596538 *in vivo*, while 3′ UTR region of *MICA* (negative control) was not immunoprecipitated with anti-SP1 antibody. To further evaluate the binding ability of SP1 to each allele *in vivo*, we sub-cloned the DNA fragment that amplified from genomic DNA of HepG2 cells before and after immunoprecipitation by anti-SP1 antibody. The subsequent sequencing results showed that 26 out of 29 tested clones contained the G allele, demonstrating the preferential binding of SP1 to the G allele (Fig. 2e).

SP1 over-expression preferentially up-regulates MICA expression at G allele

To further investigate the physiological role of the interaction between SP1 and this genomic region, we performed reporter gene assay. Three copies of 31-bp DNA fragments flanking the candidate functional SNP rs2596538 were subcloned into the multiple cloning sites of the pGL3 promoter vector. The relative luciferase activity of the plasmid including the G allele was significantly higher than that including the A allele (Fig. 3a). Furthermore, over-expression of SP1 in the cells could significantly enhance the luciferase activity of the G-allele vector, while the enhancement of the A-allele vector was relatively modest (Fig. 3a).

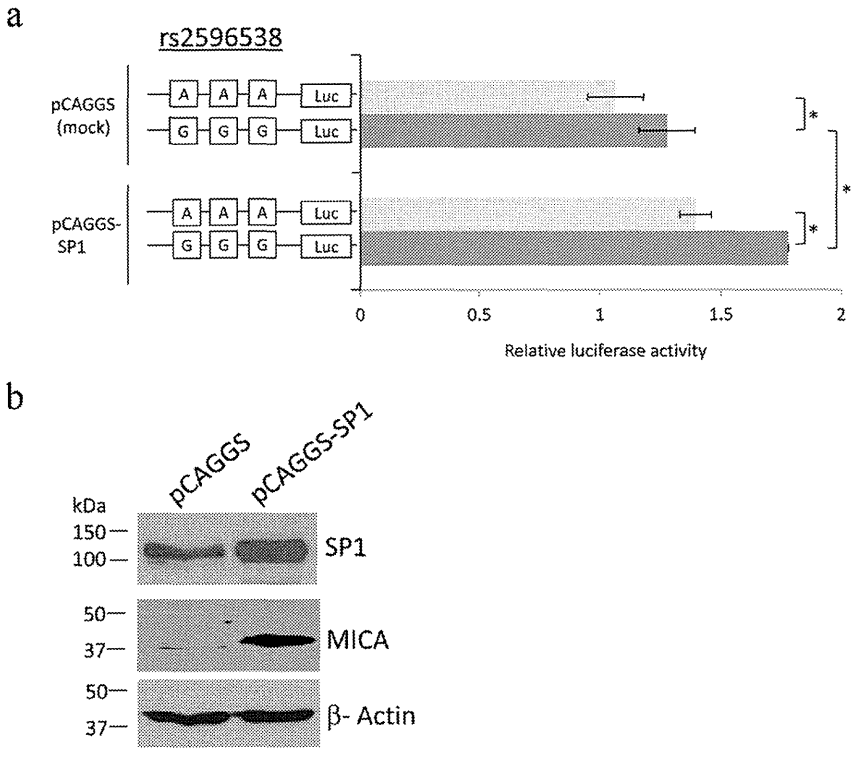

Figure 3. Transcriptional regulation of MICA by SP1 through genomic region including SNP rs2596538. (**A**) Reporter assay using constructs including 3 copies of 31 bp DNA fragment flanking SNP rs2596538. Reporter constructs are transfected into HLE cells with pRL-TK and pCAGGS or pCAGGS-SP1 vector. The value of relative luciferase activity was calculated as the firefly luciferase intensity divided by the renilla luciferase intensity. The data represent the mean ± SD value of 4 independent studies. (*$P<0.05$, Student's *t*-test) (**B**) MICA expression in HLE cells after transfection with pCAGGS or pCAGGS-SP1 vector. β-actin is served as a protein loading control.
doi:10.1371/journal.pone.0061279.g003

We also evaluated the effect of ectopically expressed SP1 on the MICA expression in HLE cells. Western-blot analysis showed that MICA protein expression was significantly increased after the SP1 over-expression (Fig. 3b). These results provided a strong evidence that the G allele has higher transcriptional potential that can be inducible by SP1.

Association of SNP rs2596538 with HCC risk and sMICA level in HCV-induced HCC patients

To further investigate the role of SNP rs2596538 in human carcinogenesis, we investigated the association of SNP rs2596538 with HCV-induced HCC in 721 HCV-HCC cases and 5,486 HCV-negative controls that had been genotyped using Illumina HumanHap610-Quad Genotyping BeadChip in our previous study [6]. We performed imputation analysis by using haplotype data from 1000 genome database [20] and found that an A allele of SNP rs2596538 was considered to be a risk allele for HCV-related HCC (Table 3, odds ratio = 1.343, $P = 1.82\times10^{-5}$). The functional SNP rs2596538 exhibited a stronger association with the HCC risk than the marker SNP rs2596542 (2.46×10^{-5}). We also analyzed the relationship between the SNP rs2596538 and the sMICA level among 246 HCV-induced HCC patients and found a significant association with the P-value of 0.00616 (Fig. 4). These results were concordant with our functional analyses in which the G allele exhibited a higher affinity to SP1 and revealed a higher transcriptional activity.

Table 3. Association of SNP rs2596542 and SNP rs2596538 with HCV-induced HCC.

SNP ID	Relative position[a]	A1	OR	*P* value
rs2596542	−4815	A	1.339	2.46×10^{-5}
rs2596538	−2778	A	1.343	1.82×10^{-5}

Note: Genotype data of 721 HCV-HCC cases and 5,486 HCV-negative controls were imputed using 1000 genomes as reference. A1, risk allele; OR, odds ratio for the risk allele calculated by considering the protective allele as a reference.
[a]Relative position to exon 1 of the *MICA* gene.
doi:10.1371/journal.pone.0061279.t003

Discussion

Approximately 160 million people (2.35% of the worldwide population) are estimated to have HCV infection [27]. Since HCV carriers have an increased risk to develop liver cirrhosis and subsequent HCC [28,29], the prediction of cancer risk is especially important for CHC patients. In our previous study, we have identified that SNP rs2596542 located in the upstream of *MICA* gene was significantly associated with the risk of HCC development among CHC patients as well as the serum level of sMICA [6]. In this study, we found that the genetic variant at SNP rs2596538 strongly affected the binding affinity of SP1. Over-expression of SP1 remarkably induced *MICA* expression in cells carrying the G allele that has a higher affinity to the SP1 binding. These findings are concordant with higher serum sMICA level among HCC patients with the G allele at SNP rs2596538. SP1 is a

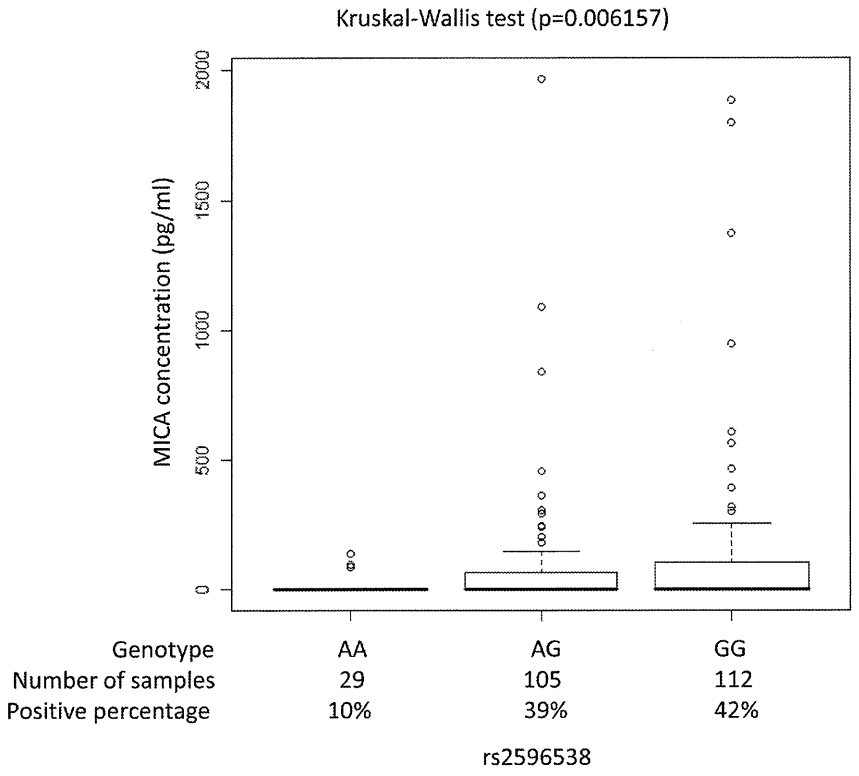

Figure 4. Association between the soluble MICA levels and SNP rs2596538 genotype. The samples were classified into 3 groups according to rs2596538 genotype. The sMICA levels measured by ELISA are indicated in y-axis. The numbers of samples and the proportion of sMICA positive subjects from each group are shown in x-axis. The percentage of the positive sMICA expression in each group are AA = 10%, AG = 39%, and GG = 42%. Statistical significance was determined by Kruskal-Wallis test.
doi:10.1371/journal.pone.0061279.g004

ubiquitously expressed transcription factor which binds to the GC-rich decanucleotide sequence (GC box) and activates the transcription of various viral and cellular genes [30,31]. Phosphorylation of SP1 was shown to be induced by HCV core protein and exhibited higher binding affinity to the promoter region of its downstream targets [32]. From our previous study, we showed a significant difference of sMICA expression between non-HCV individuals and CHC patients. This indicated that sMICA expression was induced after HCV infection [6]. Hence, we here propose the following hypothesis. After HCV infection, the virus core protein enhances the SP1 phosphorylation in hepatocytes, and the phosphorylated SP1 binds to the DNA segment corresponding to the G allele of SNP rs2596538 and then induces *MICA* expression. The membrane-bound MICA (mMICA) serves as a ligand for NKG2D to activate the immune system and results in the elimination of viral-infected cells by NK cells and CD8+ T cells [8,9]. Eventually, HCV-infected individuals with higher MICA level may cause stronger immune response to the infected cells and hence result in a reduced risk for HCC progression. Moreover, the mMICA is then shed by metalloproteinases that are often over-expressed in cancer tissues and convert mMICA to sMICA. This resulted in a significantly increase of sMICA level in the serum of HCV infected patients.

In contrast to HCV-induced HCC, our group had previously identified that higher sMICA level was associated with poor prognosis in HBV-induced HCC patients [33]. Such an opposite effect of *MICA* would be attributable to the difference in downstream pathway between HBV and HCV. HBV virus encodes hepatitis B virus X protein (HBx) that is pathogenic and promotes tumor formation. It had been reported that HBx protein was associated with an elevated expression of MT1-MMP, MMP2, and MMP3 [34,35]. HBx was also shown to transactivate MMP9 through ERKs and PI-3K-AKT/PKB pathway and suppress TIMP1 and TIMP3 activities [36,37]. The activation of metalloproteinases would induce the shedding of mMICA into sMICA, which promotes the tumor formation through the inhibitory effect of sMICA on NK cells. This can explain why high sMICA expression is a marker of poor prognosis for HBV-induced HCC. On the other hand, HCV infection was not associated with metalloproteinases activation, although the expression of sMICA was shown to be proportional to mMICA level. Therefore individuals with high MICA expression are likely to activate natural killer cells and CD8+ T cells to eliminate virus infected cells.

SP1 was previously identified as a transcriptional regulator of both *MICA* and *MICB* [7,9,38]. A polymorphism in the *MICB* promoter region was found to be associated with *MICB* transcription level [7]. To our knowledge, this is the first report showing that *MICA* transcription is directly influenced by functional variant. Moreover, this functional SNP is significantly associated with HCV-induced HCC. Our findings provide an insight that *MICA* genetic variation is a promising prognostic biomarker for CHC patients.

Supporting Information

Figure S1 Pairwise LD map between marker SNP and 11 candidates SNP. Black color boxes represent regions of high pairwise r^2 value. The LD was determined by direct DNA

sequencing of *MICA* promoter region from 50 randomly selected HCV-HCC patients.
(TIF)

Table S1 Characteristics of samples and methods used in this study.
(DOCX)

Table S2 The sequences of each oligo used in the EMSA and ChIP assay.
(DOCX)

Table S3 Copy number variation between HCV-HCC and control samples.
(DOCX)

Author Contributions

Conceived and designed the experiments: PHYL YN KM. Performed the experiments: PHYL YU VK. Analyzed the data: PHYL YU CT. Contributed reagents/materials/analysis tools: KK NK DM KC MK. Wrote the paper: PHYL KM.

References

1. Umemura T, Ichijo T, Yoshizawa K, Tanaka E, Kiyosawa K (2009) Epidemiology of hepatocellular carcinoma in Japan. J Gastroenterol 44 Suppl 19: 102–107.
2. Fassio E (2010) Hepatitis C and hepatocellular carcinoma. Ann Hepatol 9 Suppl: 119–122.
3. Mbarek H, Ochi H, Urabe Y, Kumar V, Kubo M, et al. (2011) A genome-wide association study of chronic hepatitis B identified novel risk locus in a Japanese population. Hum Mol Genet 20: 3884–3892.
4. Kamatani Y, Wattanapokayakit S, Ochi H, Kawaguchi T, Takahashi A, et al. (2009) A genome-wide association study identifies variants in the HLA-DP locus associated with chronic hepatitis B in Asians. Nat Genet 41: 591–595.
5. Zhang H, Zhai Y, Hu Z, Wu C, Qian J, et al. (2010) Genome-wide association study identifies 1p36.22 as a new susceptibility locus for hepatocellular carcinoma in chronic hepatitis B virus carriers. Nat Genet 42: 755–758.
6. Kumar V, Kato N, Urabe Y, Takahashi A, Muroyama R, et al. (2011) Genome-wide association study identifies a susceptibility locus for HCV-induced hepatocellular carcinoma. Nat Genet 43: 455–458.
7. Rodríguez-Rodero S, González S, Rodrigo L, Fernández-Morera JL, Martínez-Borra J, et al. (2007) Transcriptional regulation of MICA and MICB: a novel polymorphism in MICB promoter alters transcriptional regulation by Sp1. Eur J Immunol 37: 1938–1953.
8. Bauer S, Groh V, Wu J, Steinle A, Phillips JH, et al. (1999) Activation of NK cells and T cells by NKG2D, a receptor for stress-inducible MICA. Science 285: 727–729.
9. Zhang C, Wang Y, Zhou Z, Zhang J, Tian Z (2009) Sodium butyrate upregulates expression of NKG2D ligand MICA/B in HeLa and HepG2 cell lines and increases their susceptibility to NK lysis. Cancer Immunol Immunother 58: 1275–1285.
10. Sun D, Wang X, Zhang H, Deng L, Zhang Y (2011) MMP9 mediates MICA shedding in human osteosarcomas. Cell Biol Int 35: 569–574.
11. Waldhauer I, Goehlsdorf D, Gieseke F, Weinschenk T, Wittenbrink M, et al. (2008) Tumor-associated MICA is shed by ADAM proteases. Cancer Res 68: 6368–6376.
12. Jinushi M, Takehara T, Tatsumi T, Kanto T, Groh V, et al. (2003) Expression and role of MICA and MICB in human hepatocellular carcinomas and their regulation by retinoic acid. Int J Cancer 104: 354–361.
13. Kohga K, Takehara T, Tatsumi T, Ohkawa K, Miyagi T, et al. (2008) Serum levels of soluble major histocompatibility complex (MHC) class I-related chain A in patients with chronic liver diseases and changes during transcatheter arterial embolization for hepatocellular carcinoma. Cancer Sci 99: 1643–1649.
14. Ota M, Katsuyama Y, Mizuki N, Ando H, Furihata K, et al. (1997) Trinucleotide repeat polymorphism within exon 5 of the MICA gene (MHC class I chain-related gene A): allele frequency data in the nine population groups Japanese, Northern Han, Hui, Uygur, Kazakhstan, Iranian, Saudi Arabian, Greek and Italian. Tissue Antigens 49: 448–454.
15. Nakamura Y (2007) The BioBank Japan Project. Clin Adv Hematol Oncol 5: 696–697.
16. Tanikawa C, Urabe Y, Matsuo K, Kubo M, Takahashi A, et al. (2012) A genome-wide association study identifies two susceptibility loci for duodenal ulcer in the Japanese population. Nat Genet 44: 430–434, S431–432.
17. Miki D, Ochi H, Hayes CN, Abe H, Yoshima T, et al. (2011) Variation in the DEPDC5 locus is associated with progression to hepatocellular carcinoma in chronic hepatitis C virus carriers. Nat Genet 43: 797–800.
18. Urabe Y, Ochi H, Kato N, Kumar V, Takahashi A, et al. (2013) A genome-wide association study of HCV induced liver cirrhosis in the Japanese population identifies novel susceptibility loci at MHC region. J Hepatol.
19. Scott LJ, Mohlke KL, Bonnycastle LL, Willer CJ, Li Y, et al. (2007) A genome-wide association study of type 2 diabetes in Finns detects multiple susceptibility variants. Science 316: 1341–1345.
20. Consortium GP (2010) A map of human genome variation from population-scale sequencing. Nature 467: 1061–1073.
21. Venkataraman GM, Suciu D, Groh V, Boss JM, Spies T (2007) Promoter region architecture and transcriptional regulation of the genes for the MHC class I-related chain A and B ligands of NKG2D. J Immunol 178: 961–969.
22. Andrews NC, Faller DV (1991) A rapid micropreparation technique for extraction of DNA-binding proteins from limiting numbers of mammalian cells. Nucleic Acids Res 19: 2499.
23. Hata J, Matsuda K, Ninomiya T, Yonemoto K, Matsushita T, et al. (2007) Functional SNP in an Sp1-binding site of AGTRL1 gene is associated with susceptibility to brain infarction. Hum Mol Genet 16: 630–639.
24. Barrett JC (2009) Haploview: Visualization and analysis of SNP genotype data. Cold Spring Harb Protoc 2009: pdb.ip71.
25. Komatsu-Wakui M, Tokunaga K, Ishikawa Y, Leelayuwat C, Kashiwase K, et al. (2001) Wide distribution of the MICA-MICB null haplotype in East Asians. Tissue Antigens 57: 1–8.
26. Tse KP, Su WH, Yang ML, Cheng HY, Tsang NM, et al. (2011) A gender-specific association of CNV at 6p21.3 with NPC susceptibility. Hum Mol Genet 20: 2889–2896.
27. Negro F, Alberti A (2011) The global health burden of hepatitis C virus infection. Liver Int 31 Suppl 2: 1–3.
28. Cabibbo G, Craxi A (2010) Epidemiology, risk factors and surveillance of hepatocellular carcinoma. Eur Rev Med Pharmacol Sci 14: 352–355.
29. McGlynn KA, London WT (2011) The global epidemiology of hepatocellular carcinoma: present and future. Clin Liver Dis 15: 223–243.
30. Kadonaga JT, Tjian R (1986) Affinity purification of sequence-specific DNA binding proteins. Proc Natl Acad Sci U S A 83: 5889–5893.
31. Suske G (1999) The Sp-family of transcription factors. Gene 238: 291–300.
32. Lee S, Park U, Lee YI (2001) Hepatitis C virus core protein transactivates insulin-like growth factor II gene transcription through acting concurrently on Egr1 and Sp1 sites. Virology 283: 167–177.
33. Kumar V, Yi Lo PH, Sawai H, Kato N, Takahashi A, et al. (2012) Soluble MICA and a MICA Variation as Possible Prognostic Biomarkers for HBV-Induced Hepatocellular Carcinoma. PLoS One 7: e44743.
34. Ou DP, Tao YM, Tang FQ, Yang LY (2007) The hepatitis B virus X protein promotes hepatocellular carcinoma metastasis by upregulation of matrix metalloproteinases. Int J Cancer 120: 1208–1214.
35. Yu FL, Liu HJ, Lee JW, Liao MH, Shih WL (2005) Hepatitis B virus X protein promotes cell migration by inducing matrix metalloproteinase-3. J Hepatol 42: 520–527.
36. Chung TW, Lee YC, Kim CH (2004) Hepatitis B viral HBx induces matrix metalloproteinase-9 gene expression through activation of ERK and PI-3K/AKT pathways: involvement of invasive potential. FASEB J 18: 1123–1125.
37. Kim JR, Kim CH (2004) Association of a high activity of matrix metalloproteinase-9 to low levels of tissue inhibitors of metalloproteinase-1 and -3 in human hepatitis B-viral hepatoma cells. Int J Biochem Cell Biol 36: 2293–2306.
38. Andresen L, Jensen H, Pedersen MT, Hansen KA, Skov S (2007) Molecular regulation of MHC class I chain-related protein A expression after HDAC-inhibitor treatment of Jurkat T cells. J Immunol 179: 8235–8242.